Pergamon

Journal of Structural Geology, Vol. 17, No. 3, pp. 305 to 328, 1995

0191-8141/95 $9.50+0.00

0191-8141(94)00057-3

Polyphase deformation in the western Mount Isa Inlier, Australia: episodic or continuous deformation?

KAREN A. CONNORS* and GORDON S. LISTER

Victorian Institute of Earth and Planetary Sciences, Department of Earth Sciences, Monash University, Clayton, Victoria 3168, Australia

(*Received* 19 *December* 1991; *accepted in revised form* 26 *April* 1994)

Abstract—The polyphase deformation history of the Mount Novit Ranges, western Mount Isa Inlier, Australia, involved the development of four generations of N–S to NW-plunging folds, development of which alternated with movement on ~N–S striking faults/shear zones with west-over-east displacement. The spatial relationships between successive structures and the distinct similarities in the kinematics, style, and asymmetry, are all consistent with continuous deformation during E–W to NE–SW shortening. Additional support for this hypothesis is based on the development of the three major fold generations, and the intervening faults and shear zones, during low-*P*, high-*T* metamorphism. Although the duration of this metamorphic event cannot be constrained, recent studies have linked low-*P* metamorphism to heat advection by migrating melts. Thermal modelling indicates that such metamorphic events will be short-lived in comparison to those associated with thermal relaxation of over-thickened crust. Low-*P* metamorphism is unlikely to persist through two or more separate tectonic events; therefore syn-metamorphic, polyphase deformation in the Mount Novit Ranges apparently formed during a single, continuous tectonic episode.

This structural history differs from both the regional scheme and that of previous workers in this area. The main differences are: (i) no evidence was found for early thrust faulting prior to N–S folding; (ii) there are four generations of N–S to NW–SE folds, as opposed to two; and (iii) this study favors a single, consistent tectonic regime, in contrast to the interpretation of three discrete, isolated tectonic events.

INTRODUCTION

Regional correlations in the Mount Isa Inlier of Australia have resulted in a simplified structural history including: D_1 south-directed thrust faults and east–west folds; D_2 north–south folds and cleavages; and D_3 north-northwest folds and cleavages (Bell 1983, Blake 1987). The ages of these three tectonic events have been interpreted as 1610 ± 13 Ma, 1544 ± 12 Ma and 1510 ± 13 Ma, based on Rb–Sr whole rock analyses and supposed identification of S_1, S_2, and S_3 domains (Page & Bell 1986) within the ~1657 Ma Sybella Batholith (Connors & Page 1992, in press) (Fig. 1). These three events have therefore been considered as discrete episodes of deformation related to isolated tectonic events (e.g. Blake 1987, Bell 1991, Bell *et al.* 1992) which are separated by substantial time breaks (i.e. ~66 Ma and ~34 Ma).

This simplified deformation scheme has been applied throughout the inlier, and has resulted in the misleading impression of a direct correlation between observed structural generations and crustal deformation episodes (i.e. all D_1 structures formed contemporaneously throughout the inlier as a result of the D_1 orogenic event; Holcombe & Stewart 1992). In addition, there are conflicting interpretations of the early low-angle faults which have cast doubt over the regional significance of postulated D_1 thrusting. Further questions about the general applicability of the D_1–D_2–D_3 scheme and the accuracy of the Rb–Sr deformation ages have arisen recently. The main issues of this controversy can be summarized as follows.

(1) Bell (1983, 1991) has postulated that D_1 thrusting is a regionally significant event, and several workers have presented evidence for early thrust faulting in local areas (e.g. Loosveld & Schreurs 1987, Blake 1992, Hill *et al.* 1992, Loosveld 1992, Nijman *et al.* 1992, Stewart 1992a). Numerous structures interpreted as D_1 thrust faults and imbricates, however, have been interpreted by other workers as extensional faults (e.g. Smith 1969, Dunnet 1976, Derrick 1982, Passchier 1986, Pearson *et al.* 1987, 1992, Passchier & Williams 1989, Proffett 1989, 1990, Stewart 1989, 1992b, Williams 1989, Holcombe *et al.* 1991, Bain *et al.* 1992, Nijman *et al.* 1992, among others) or as younger (post-'D_2') thrust faults (Connors 1989, 1992, Huang 1990, 1991, Connors *et al.* 1992). Furthermore, many detailed studies have failed to identify any compressional structures, other than minor folds or cleavages, that pre-date the oldest north–south folds (i.e.'D_2') (Passchier 1986, Pearson *et al.* 1987, 1992, Passchier & Williams, 1989, Stewart 1989, Williams 1989, Holcombe *et al.* 1991, Oliver *et al.* 1991, Connors *et al.* 1992, this study). Although early thrusting occurred, at least in some areas, it is difficult to support a regionally significant period of early thrust faulting based on the present data. It is possible that many pre-'D_2' structures are extensional.

(2) The regional north–south folds are commonly interpreted as D_2 (e.g. Bell 1983, Blake 1987) and are used as a marker event to determine the relative ages of other structures. Problems with correlation are

*Present address: Geological Survey of Canada, 601 Booth St., Ottawa, Ontario, Canada, K1A 0E8.

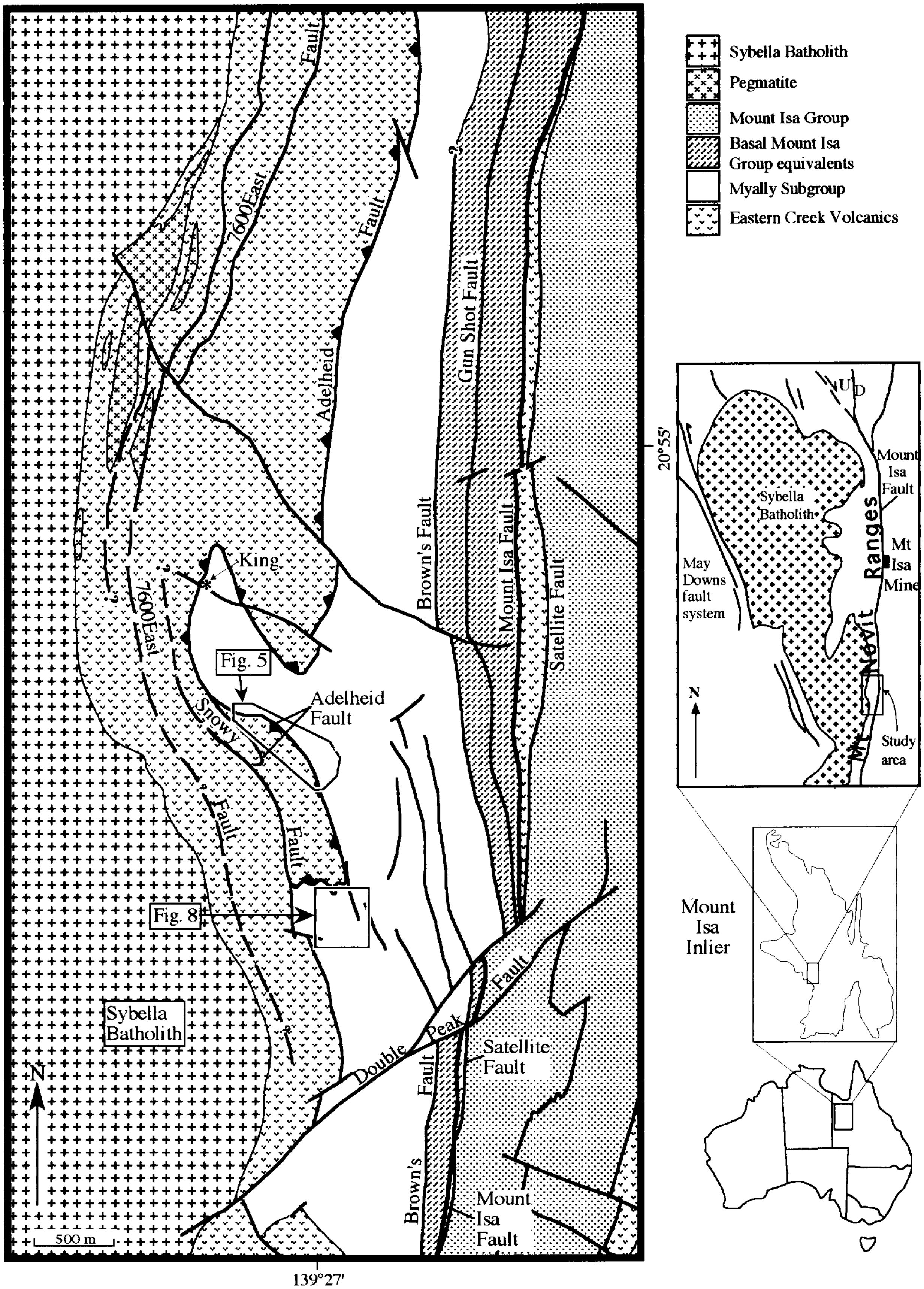

Fig. 1. Simplified map of the southern Mount Novit Ranges showing distribution of the main units and location of major faults. Small scale maps on right show the location of the study area within the Mount Isa Inlier. Locations of Figs. 5 and 8 are indicated.

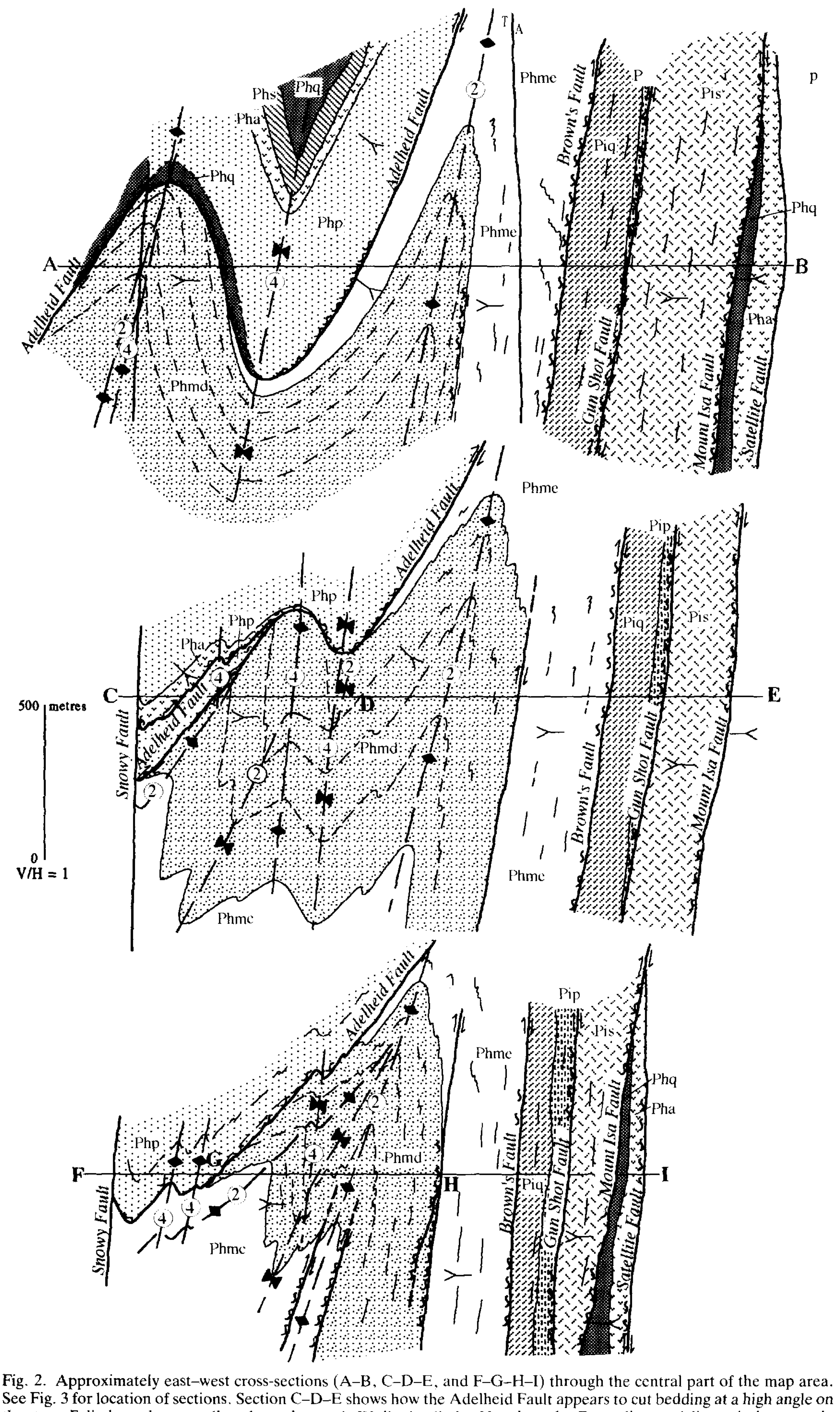

Fig. 2. Approximately east–west cross-sections (A–B, C–D–E, and F–G–H–I) through the central part of the map area. See Fig. 3 for location of sections. Section C–D–E shows how the Adelheid Fault appears to cut bedding at a high angle on the steep F_2 limbs and at a small angle on the gentle W-dipping limbs. Note how the F_4 syncline–anticline pair decreases in amplitude and dies out to the south (from A–B to F–G–H–I).

inevitable, however, because there is more than one generation of north–south folds in many areas (e.g. Winsor 1986, Stewart 1989, Connors 1992). Therefore regional north–south folds cannot be interpreted as D_2 and older structures cannot be considered as D_1, without detailed mapping and geometrical analyses.

(3) Further doubt concerning the D_1–D_2–D_3 scheme and the age of deformation is provided by form surface mapping of cleavages within the Sybella Batholith (BMR 1978, Proffett 1990, Connors *et al.* 1991, 1992) and new U–Pb geochronological data (Connors 1992, Connors & Page 1992, in press) which indicates that the ~1610 Ma Rb–Sr age for D_1 (Page & Bell 1986) represents partial resetting during D_2 and cannot date D_1 thrusting.

This paper presents the results of a detailed structural study in the Mount Novit Ranges (Fig. 1). Several features of this area make it key to the understanding of the structural/tectonic history of the western inlier. First, a major D_1 roof thrust has been postulated, therefore this hypothesis can be tested. Second, differing interpretations have been presented for the structural history of this area and the surrounding region (e.g. Lister 1969, Wilson 1975, Winsor 1986, Profett 1990, Bell 1991). Third, it occurs adjacent to the Sybella Batholith from which Page & Bell (1986) obtained the D_1–D_2–D_3 ages, so these results can be evaluated. In addition, the Mount Novit Ranges are juxtaposed with the mineralized Mount Isa Group rocks; therefore a better understanding of the structural history may aid future exploration.

The D_1–D_2–D_3 terminology used above refers to the regional scheme, whereas the F_1/S_1–F_2/S_2–S_{3a}/L_{3a}–F_{3b}/S_{3b}–F_4/S_4–F_5/S_5 terminology below will refer to the Mount Novit Ranges. No correlations are implied.

STRUCTURAL HISTORY OF THE MOUNT NOVIT RANGES

The Mount Novit Ranges (Fig. 1) are dominated by mafic metavolcanic rocks of the Eastern Creek Volcanics (~1780–1740 Ma) and metasediments of both the Myally Subgroup and lower Mount Isa Group equivalents (1653 ± 7 Ma; R. W. Page unpublished data). The ranges are bounded to the west by the Sybella Batholith and to the east by the Mount Isa Fault. Although many workers have studied various aspects of the area surrounding the Cu and Pb–Zn deposits at Mount Isa (Fig. 1), only a few studies have focused on the structure of the higher grade rocks of the Mount Novit Ranges which are faulted against the ore-bearing Mount Isa Group. Although mapping by Carter *et al.* (1961) and Hill *et al.* (1975) included the Mount Novit Ranges, these regional studies did not focus on the structural history. The first detailed structural studies documented evidence for three to four fold generations and numerous faults and shear zones (Lister 1969, Wilson 1972, 1973, 1975). Possible thrust faults were first recognized in the mine area by Williams (1970). More recently, Bell (1991) postulated a major D_1 roof thrust (based in part on the work of Adelheid Weniger, unpublished data) with >250 km of south-directed movement which was overprinted by north–south upright D_2 folds and later north-northwest D_3 folds. Bell (1991) alluded to the development of multiple cleavages during D_2 and D_3, but did not provide much detail.

Bell's D_1 thrust faults represent one of the main points of debate in the Mount Novit Ranges and the surrounding Mount Isa area. Downing (1986) and Bell (1983, 1991) postulated D_1 thrusting in the Mount Novit Ranges west of the Mount Isa Fault, whereas Proffett (1989, 1990), Davoren (1991), Huang (1990, 1991) and Connors *et al.* (1992) have not found evidence of early thrust faulting.

The present study indicates that the structural history of the Mount Novit Ranges involved intermittent folding and faulting which differs significantly from the D_1–D_2–D_3 scheme of Bell (1983, 1991). The structural history of this study area is described below with reference to the map (Fig. 3) and cross-sections (Fig. 2) which highlight the large scale structures, and to Fig. 4 which summarizes the sequence of events. This section is followed by a detailed description of the mesoscopic and microscopic overprinting relationships at several key locations.

F_2 folds and S_2 schistosity occur throughout the area and represent the most pervasive stage of deformation. The folds are asymmetrical with gently-dipping western limbs and steeply overturned eastern limbs (Fig. 4a). These structures overprint an older cleavage, but there is little evidence of older macroscopic structures.

F_2 folding was followed by west-over-east movement on ductile faults and shear zones such as the Mount Isa and Adelheid Faults (Figs. 2 and 4b). The Mount Isa Fault formed on the attenuated, overturned limb of the N-plunging F_2 anticline (Figs. 2 and 4b). At the same time, the Adelheid Fault formed subparallel to bedding on the more gently W-dipping limbs of the large scale F_2 folds and cut across bedding at a high angle on the more steeply-dipping overturned limbs (Figs. 2 and 4b). The Adelheid Fault is not folded by either of the two largest F_2 folds despite the fact that it is subparallel to bedding along much of its length (Figs. 2 and 3). The fault cuts the western limbs of both folds, but it is not repeated on the eastern limbs (Figs. 2 and 3). Therefore the fault is either the same age as the F_2 folds or younger; it cannot be part of an older roof thrust as proposed by Bell (1991).

Brown's Fault, the Gun Shot Fault and several shear

Fig. 3. Geologic map of the study area reduced from 1:5000 scale field map. Note overprinting relationships between large scale folds and faults. The Adelheid Fault (AF) truncates F_2 folds (at Location 2 in Fig. 5 and just north of the map) and is folded by F_4. F_4 folds are in turn truncated by the Snowy Fault and the 7600 East Fault.

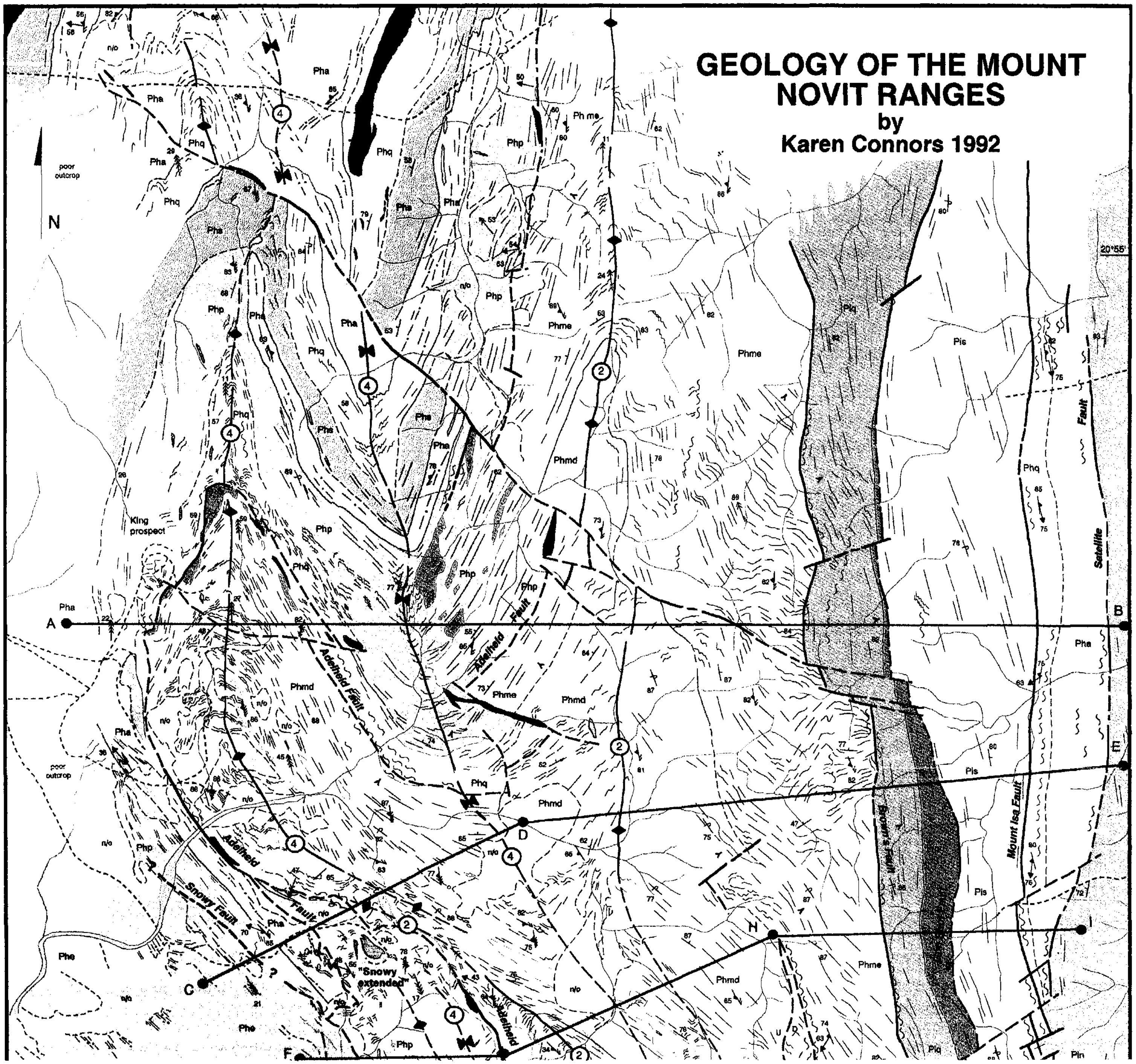
GEOLOGY OF THE MOUNT
NOVIT RANGES
by
Karen Connors 1992
N
poor outcrop
King prospect
Adelheid Fault
Snowy Fault
Brown's Fault
Mount Isa Fault
Satellite Fault
"Snowy extended"
20°55'
A
B
C
D
E
F
H
I

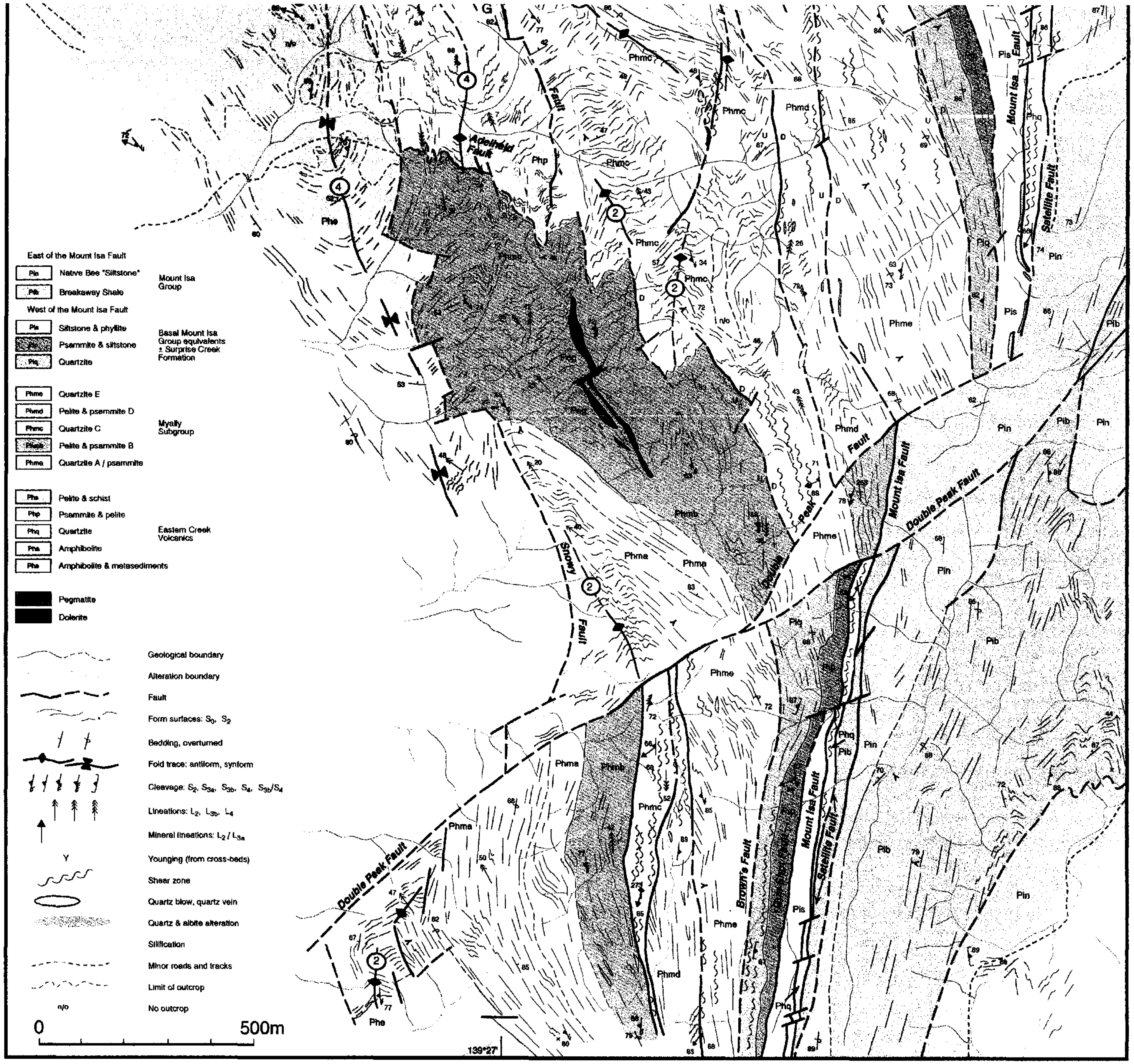

East of the Mount Isa Fault
Pin Native Bee "Siltstone"
Pib Breakaway Shale
Mount Isa Group
West of the Mount Isa Fault
Pis Siltstone & phyllite
Pip Psammite & siltstone
Piq Quartzite
Basal Mount Isa Group equivalents ± Surprise Creek Formation
Phme Quartzite E
Phmd Pelite & psammite D
Phmc Quartzite C
Phmb Pelite & psammite B
Phma Quartzite A / psammite
Myally Subgroup
Phe Pelite & schist
Php Psammite & pelite
Phq Quartzite
Pha Amphibolite
Pha Amphibolite & metasediments
Eastern Creek Volcanics
Pegmatite
Dolerite
Geological boundary
Alteration boundary
Fault
Form surfaces: S_0, S_2
Bedding, overturned
Fold trace: antiform, synform
Cleavage: S_2, S_{3a}, S_{3b}, S_4, S_{3b}/S_4
Lineations: L_2, L_{3b}, L_4
Mineral lineations: L_2 / L_{3a}
Younging (from cross-beds)
Shear zone
Quartz blow, quartz vein
Quartz & albite alteration
Silicification
Minor roads and tracks
Limit of outcrop
No outcrop
0
500m
Mount Isa Fault
Satellite Fault
Double Peak Fault
Brown's Fault
Snowy Fault
Adelheid Fault
139°27'

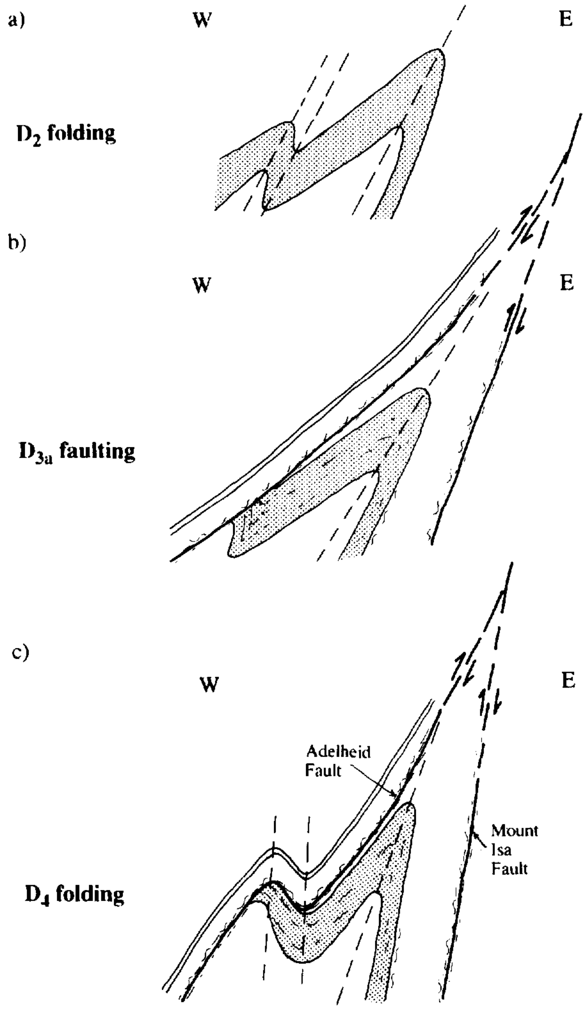

Fig. 4. Simplified cross-sections depicting the effects of the three principal deformation phases in the Mount Novit Ranges. Stippled unit represents the psammite + pelite unit D of the Myally Subgroup which is both overlain and underlain by quartzite. The final schematic section represents a simplified version of the detailed cross-sections of Fig. 2. See text for further details.

zones along major contacts, occur subparallel to the Mount Isa Fault (Fig. 1). Overprinting relationships indicate that these structures were active at the same time. Deformation intensifies to the south along these structures and many units are significantly thinned (Figs. 1 and 3). South of Double Peak Fault some units are reduced to 25% of their thickness farther north.

The post-F_2 ductile faults and shear zones are closely associated with F_{3b} folds. These folds are strongly asymmetrical and highly non-cylindrical close to the faults and shear zones, but they become more upright, less asymmetrical and gently doubly-plunging, and S_{3b} decreases in intensity, away from the faults. The heterogeneous nature of F_{3b}/S_{3b} and associated faults has resulted in domains of intense deformation separated by areas where F_2/S_2 structures are well preserved.

Continued movement on the faults/shear zones during and after F_{3b} folding is demonstrated by truncation of folds which are correlated with D_{3b} of this study (Connors *et al.* 1992), by the W-dipping, west-block-up Mica Creek Shear Zone and Big Beryl Fault which are exposed 15 km to the north (Proffett 1989). In addition, microstructures from the Mount Isa and Adelheid faults demonstrate post-F_{3b} movement (see below).

The overprinting effects of F_4 folding vary due to the orientation of older structures. This phase of shortening had little effect on the moderately to steeply dipping Mount Isa Fault or the overturned limbs of the F_2 folds, except for steepening of the faults and axial planes, and tightening of the folds (Fig. 4c). In general, the F_2 folds are not refolded because their axial planes and eastern limbs were quite steep and because, in some areas, F_2 and F_4 folds are nearly coaxial. The effects of F_4 are most obvious on the gently dipping limbs of the F_2 folds and the Adelheid Fault. Note that the large scale F_4 anticline–syncline pair was localized by the older F_2 anticline–syncline pair, and that F_4 folding caused the F_2 syncline to open out (Fig. 4). The F_4 fold pair dies out to the south due to interference with the steep, WNW-trending limb of the older F_2 fold (Figs. 2 and 3). F_4 folding was followed by further west-block-up faulting (Snowy Fault; Fig. 2) and by minor NW-plunging F_5 folding.

Although the map scale structures demonstrate several key overprinting relationships, many questions concerning the structural history of the Mount Novit Ranges and the relationship between deformation and metamorphism remain unanswered. Therefore the following section is used both to describe the detailed mesoscopic and microstructural overprinting relationships and to show the links between these outcrop scale features and the map scale structures.

Microstructures and mesoscopic overprinting relationships

As is the case in most multiply deformed terrains, unequivocal overprinting relationships are found only in some outcrops. Careful geometric analyses of these outcrops, correlation with the map scale structures and extrapolation to adjacent areas has proved to be of fundamental importance. In the Mount Novit Ranges, this analysis of fabrics and microstructures has allowed interpretation and identification of the different generations of structures, and identified key relationships that can be used for correlation across the area. Extrapolation and correlation have been based on: (1) overprinting relationships; (2) form surface mapping which allows tracing of the structural elements between outcrops; and (3) distinguishing characteristics of structural elements. Three key locations will be described.

Location 1. The NE-verging F_2 fold has a gently SW-dipping upper limb and a steeply overturned lower limb (Fig. 5). The S_0/S_2 intersection lineation and F_2 fold axes plunge gently west-northwest to northwest. The pervasive S_2 axial planar schistosity dips moderately southwest to west-southwest and is the dominant fabric. In psammitic layers, S_2 is a finely spaced cleavage defined by oriented micas (Fig. 6a), and in mica rich units, it forms a finely differentiated schistosity (0.25–0.5 mm).

In thin section, straight, strain-free laths of intergrown muscovite and biotite are largely aligned parallel to the S_2 schistosity, but many lie at high angles, displaying a decussate texture (criss-cross pattern; Fig. 6a) which is best developed in the more micaceous units (Fig. 6b). In the psammopelite units, quartz grains display undulose extinction or prismatic subgrains, imposed on granoblastic textures. Single quartz grains fill the spaces between adjacent mica laths suggesting that continued grain growth was restricted by the presence of mica (Fig. 6a). These recrystallization microstructures which minimize surface free energy, reflect post-S_2 annealing.

The decussate micas oriented at an angle to the S_2 schistosity (Figs. 6a & b) preserve crenulations of an older fabric. This pre-S_2 fabric is also preserved as inclusion trails in porphyroblasts. The inclusion trails are generally straight and vary in orientation with respect to the external S_2 cleavage which is deflected around the porphyroblasts. This pre-S_2 fabric may represent either a tectonic foliation or a depositional fabric. No F_1 folds have been documented.

Although the mineral lineation, S_0/S_2 intersection, and F_2 fold axes all plunge west-northwest at this location, F_2 folds and the L_2 mineral lineation both vary in orientation. In general, L_2 is sub-parallel to W- to NW-plunging F_2 fold axes, but is at a large angle to N-trending F_2 folds. This fold–lineation relationship suggests that at least some of the variation in F_2 orientation originated during F_2; however, part may result from later deformation.

The observations from this location demonstrate: (i) the existence of an older, although enigmatic, fabric; and (ii) the nature of the S_2 cleavage, its link to the map scale F_2 folds and its timing with respect to metamorphism. This S_2 cleavage can be traced to the northwest, by form surface mapping, into Location 2 where it is overprinted by several phases of deformation (Figs. 3 and 5).

Location 2. The W-dipping Adelheid Fault places the Eastern Creek Volcanics over younger Myally Subgroup (Figs. 1, 3 and 5). A zone of intense deformation and alteration defines the fault. The alteration assemblages (coarse quartz ± white mica ± chlorite, chlorite or biotite ± feldspar ± quartz, and chlorite ± biotite ± white mica) obscure the original wall rocks and locally extend 150 m from the fault. Timing relationships are also obscured; however, in less altered zones, the phyllosilicates grow across S_2 indicating post-S_2 alteration, in agreement with map scale overprinting relationships.

Two generations of structures have developed in association with the Adelheid Fault. The older generation, S_{3a}, is largely confined to a 5–15 m wide zone and is associated with a strong L_{3a} mineral lineation. In altered rocks, S_{3a} is defined by thin chlorite seams and variations in grain size (Fig. 6c). Thin bands (less than 0.5 mm) of fine, recrystallized quartz (0.01–0.05 mm) separate bands of coarse grained quartz with a more variable grain size (0.05–2.5 mm). In the coarse grained bands, the grains are irregularly shaped with strongly sutured boundaries and contain subgrains and deformation lamellae. Recrystallized grains (0.05 mm) occur along grain boundaries. A grain shape fabric oblique to S_{3a} indicates west-over-east movement (Fig. 6c). These microstructures indicate that temperature was insufficient for quartz recrystallization during the final stages of fault movement.

S_{3a} is overprinted by S_{3b} and F_{3b} folds. Adjacent to the Adelheid Fault, E- to NE-verging F_{3b} folds are tight, strongly asymmetrical and highly non-cylindrical. There is marked variation in fold axis orientation within the axial plane, ranging from subhorizontal to steep plunges, and trending from northwest to north and southeast to south. These folds have elongate elliptical sections in the YZ plane and approach a sheath fold geometry. The sheath axes plunge west–southwest parallel to the L_{3a} mineral lineation. Away from the fault, F_{3b} folds become more upright and more cylindrical, and the intensity of S_{3b} decreases.

S_{3b} is commonly a coarse (3–10 mm), discrete crenulation cleavage (terminology after Gray 1977) which approaches a differentiated layering (Fig. 6d). S_{3b} is defined by septa of intergrown muscovite and biotite (Fig. 6d). S_2 cleavage traces within microlithons truncate against (001) boundaries of septa micas (Figs. 6d & e). Quartz grains show undulose extinction, subgrains, and smooth to lobate boundaries, and mica laths are generally straight and unstrained with length to width ratios on the order of 10:1. Although these textures indicate that temperature was sufficient for post-S_{3b} mica recrystallization, there is no evidence for significant grain growth of mica or quartz after S_{3b}. In local zones, S_{3b} is an intense, pervasive cleavage that is difficult to distinguish from S_2.

S_{3b} can be traced to the northwest where it is in turn overprinted by steep F_4/S_4 structures (Figs. 5 and 7). This S_4 cleavage can be traced north to the core of a large scale anticline (Fig. 3) therefore demonstrating that this north–south anticline is an F_4 fold which post dates similarly oriented F_2 folds. This agrees with map scale relationships which show that the Adelheid Fault is folded by the F_4 fold pair.

Mesoscopic F_4 folds are non-cylindrical and S_4 is a steep, zonal crenulation cleavage (terminology after Gray 1977) (Fig. 6f). In thin section, the crenulations and cleavage are defined by bent, deformed mica laths and strained quartz grains displaying undulose extinction, sutured boundaries, and subgrain development (Fig. 6f). This implies that temperature was insufficient for recrystallization of mica and quartz after S_4 development, with the exception of local zones of weak recrystallization.

Observations at this location demonstrate that S_2 which is axial planar to the F_2 anticline at Location 1 is overprinted by the Adelheid Fault and F_{3b}/S_{3b}, and that all of these structures are in turn overprinted by the north–south F_4 folds. The quartz and mica microstructures suggest that S_2, S_{3b} and S_4 developed at progressively lower grade metamorphic conditions.

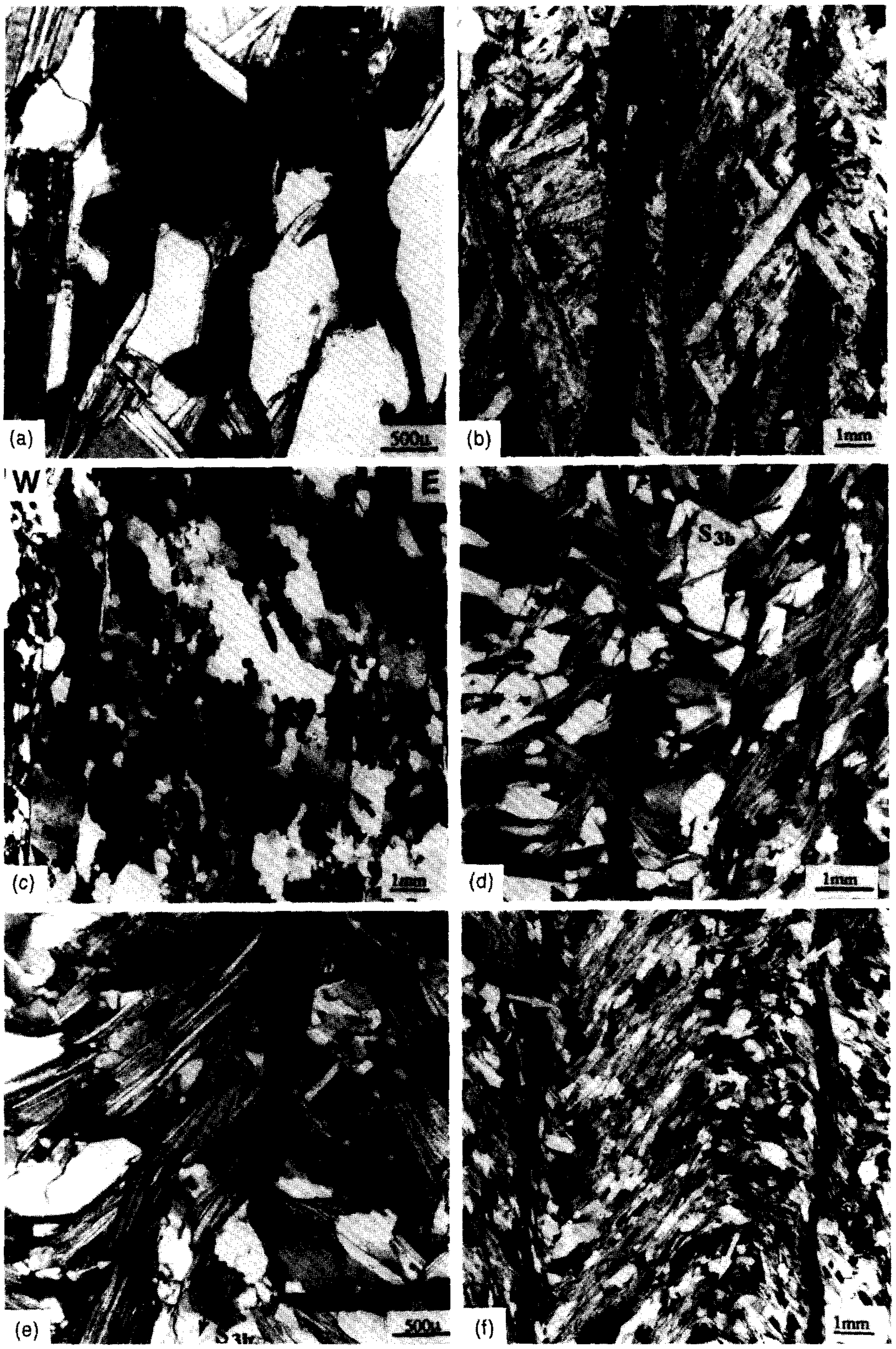

Fig. 6. (a) Photomicrograph of S_2 in psammopelite from near the hinge of the large scale. NW-plunging F_2 fold shown in Fig. 5. Intergrown biotite and muscovite form straight, strain-free laths which preserve crenulations of an older fabric (e.g. cross micas within quartz-rich microlithons). Biotite typically forms broad laths with smaller $l:w$ ratios than muscovite. Quartz grains are elongate parallel to S_2 and some show undulose extinction, but there is no evidence of grain boundary migration. Single quartz grains fill spaces between micaceous septa. (Thin section cut perpendicular to S_2 and L_2 intersection lineation.) (b) Photomicrograph of S_2 in pelite from near the hinge of the large scale, N-plunging F_2 anticline of Fig. 3. Note the better preservation of the older crenulated fabric within the more micaceous unit. (Thin section cut perpendicular to S_2 and L_2 intersection lineation). (c) Photomicrograph of S_{3a} (near vertical fabric) in quartz-rich, altered rock of the Adelheid Fault zone. S_{3a} is defined by thin seams of chlorite (black arrows) and alternating bands of fine and coarse grained quartz (white arrow). Note grain shape fabric indicating west-block-up displacement. (Thin section cut perpendicular to S_{3a} and parallel to L_{3a} mineral lineation.) (d) Photomicrograph of S_{3b} discrete crenulation cleavage (near vertical fabric) in psammopelite from Location 2. Intergrown biotite and muscovite defining S_2 cleavage traces in the microlithons, are truncated by micas aligned parallel to S_{3b}. Although the extinction is undulose and subgrains have developed in restricted areas, single quartz grains fill the spacing between S_2 septa similar to Location 1. (Thin section cut perpendicular to S_{3b} and L_{3b} crenulations.) (e) Enlarged view of S_{3b}. Septa micas truncate microlithon micas defining S_2. Note F_4 kinks and crenulations (indicated by white arrows) overprinting S_{3b} and resulting in undulose extinction in the quartz. (Thin section cut perpendicular to S_3 and L_{3b} crenulations.) (f) Photomicrograph of L_4 crenulations and incipient S_4 zonal crenulation cleavage. The micas, which have large length to width ratios, are bent and show undulose extinction. Quartz grains also show strong undulose extinction. (Thin section cut perpendicular to L_4 crenulations.) All photomicrographs were taken with crossed polars.

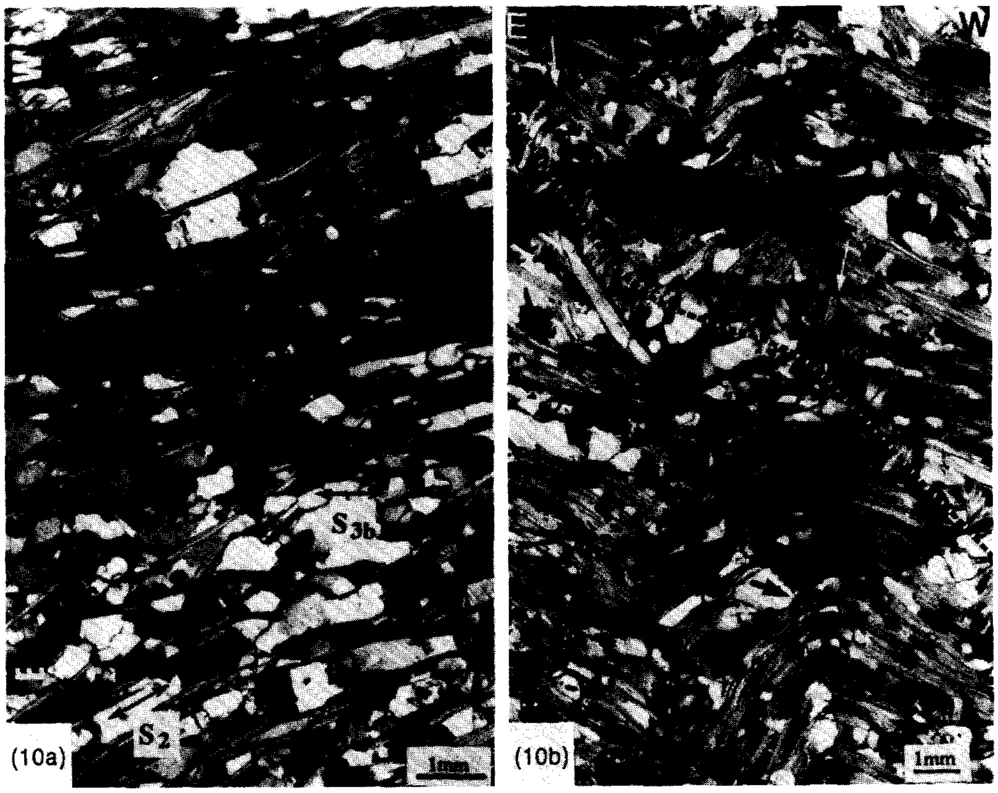

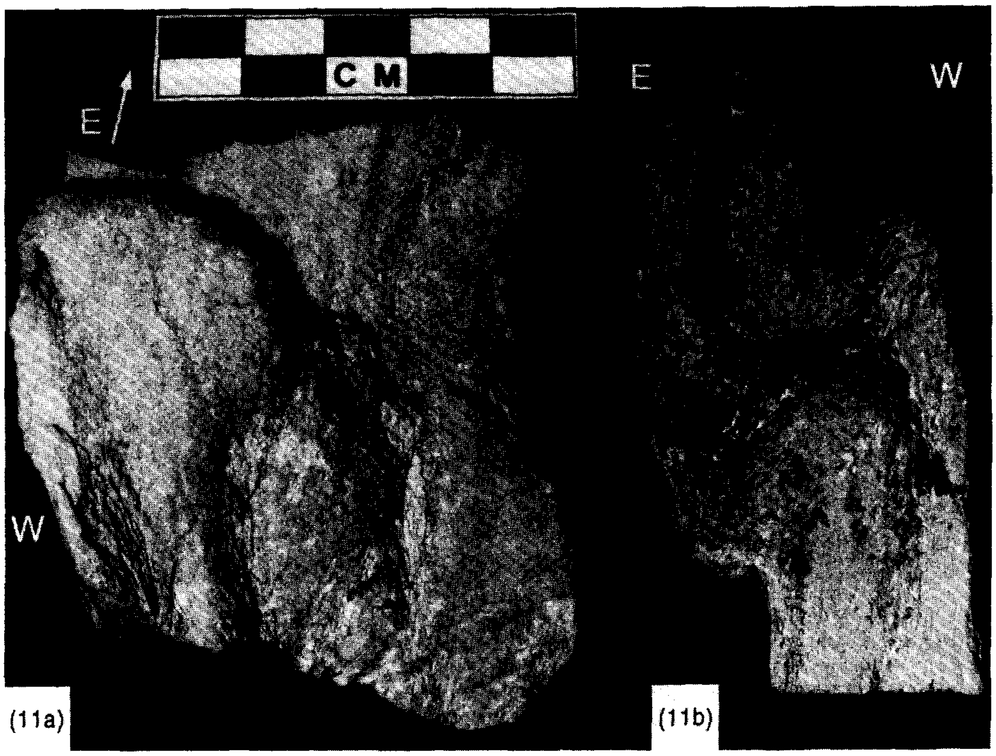

Fig. 10. (a) Photomicrograph of weakly differentiated, steep S_{3b} (horizontal in photo) overprinting W-dipping S_2 at Location 3a (see Fig. 9a for orientation of photo relative to mesoscopic structures). The S_{3b} cleavage zones are defined by the zones of darker (near extinction) micas in the centre and the top of the photo. Spacing of cleavage zones is similar to S_{3b} at Location 2, but the degree of differentiation is significantly lower. Recrystallized textures of quartz and mica defining S_2 are still evident. (Thin section cut perpendicular to S_{3b} and S_{3b}/S_2 intersection.) (b) Photomicrograph of S_{3b}/L_{3b} (folded) and S_4/L_4 (near vertical) crenulations overprinting S_2. The trace of the folded S_{3b}/L_{3b} is indicated by the dashed line. (Thin section cut perpendicular to L_4 crenulation axes.) Both photos are taken with crossed polars.

Fig. 11. (a) & (b) Asymmetrical, non-cylindrical F_{3b} folds from the hanging wall of the Mount Isa Fault. Note the curvature of the fold hinge in (a).

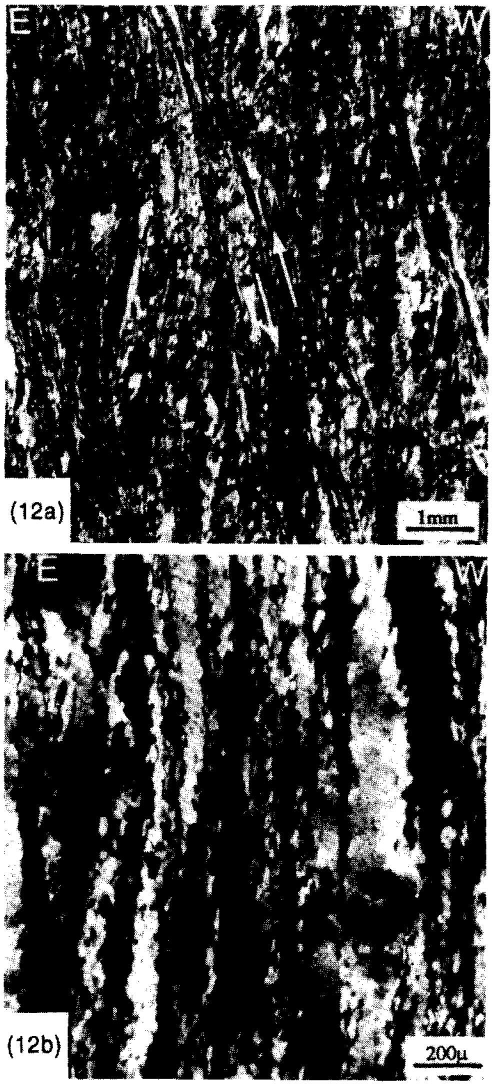

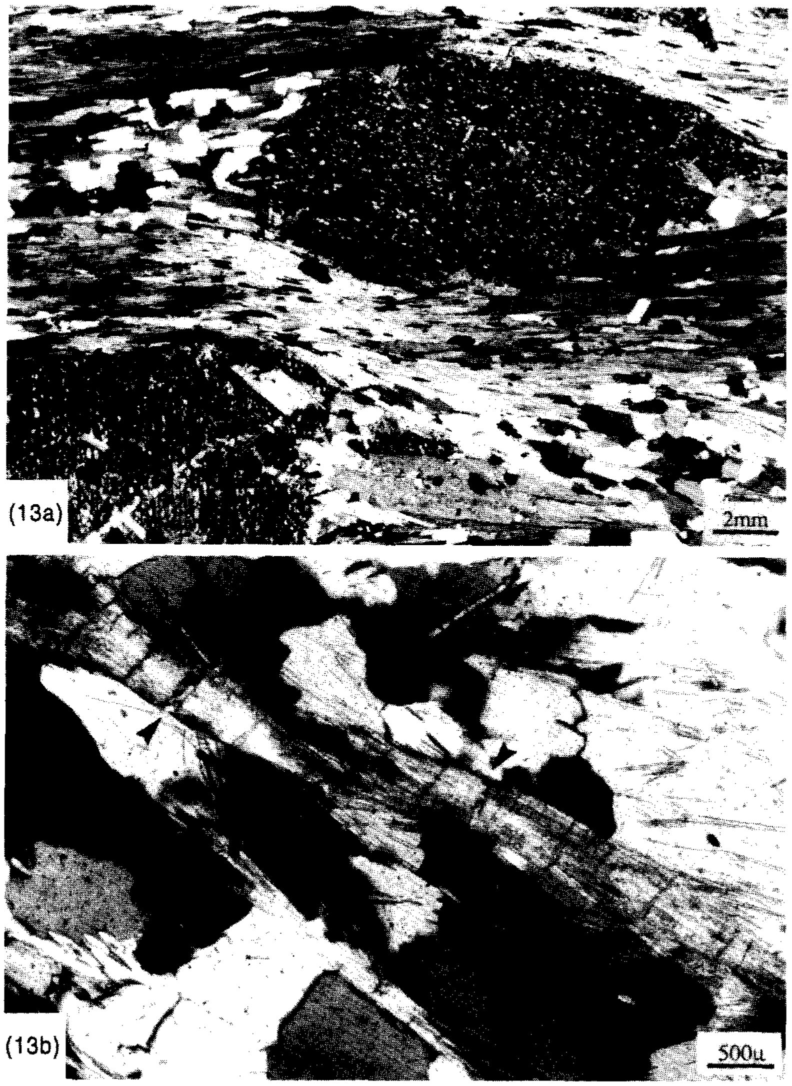

Fig. 12. (a) & (b) Microstructures in mylonites of the Mount Isa Fault. S_{3a} (vertical) is defined by thin seams of micas and opaque minerals, and by elongate quartz grains or 'families' of quartz grains of similar optical orientation. (a) Note development of the shear bands indicating west-over-east movement. (b) '*C*' planes (defined by prismatic subgrains) also demonstrate west-over-east sense of shear. (Both thin sections cut perpendicular to S_{3a} and parallel to L_{3a}.) Both photos are taken with crossed polars.

Fig. 13. (a) Photomicrograph showing deflection of S_2 around cordierite porphyroblasts and development of strain shadows adjacent to the porphyroblasts. Note recrystallized textures of quartz and mica within the strain shadow, and variations in the orientation of inclusion trails (S_1?) within the porphyroblasts. (Thin section cut perpendicular to S_2.) (b) Photomicrograph of stretched bundles of fibrolite defining the L_{3a} mineral lineation in the footwall of the Adelheid Fault at the King prospect (see Fig. 1 for location). Fractures in fibrolite bundles are oriented perpendicular to the extension direction and are filled by white mica (arrowheads). Quartz microstructures show granoblastic textures with triple junctions and boundaries vary from smooth to sutured. (Thin sections cut parallel to L_{3a} and perpendicular to S_{3a}.) Both photos are taken with crossed polars.

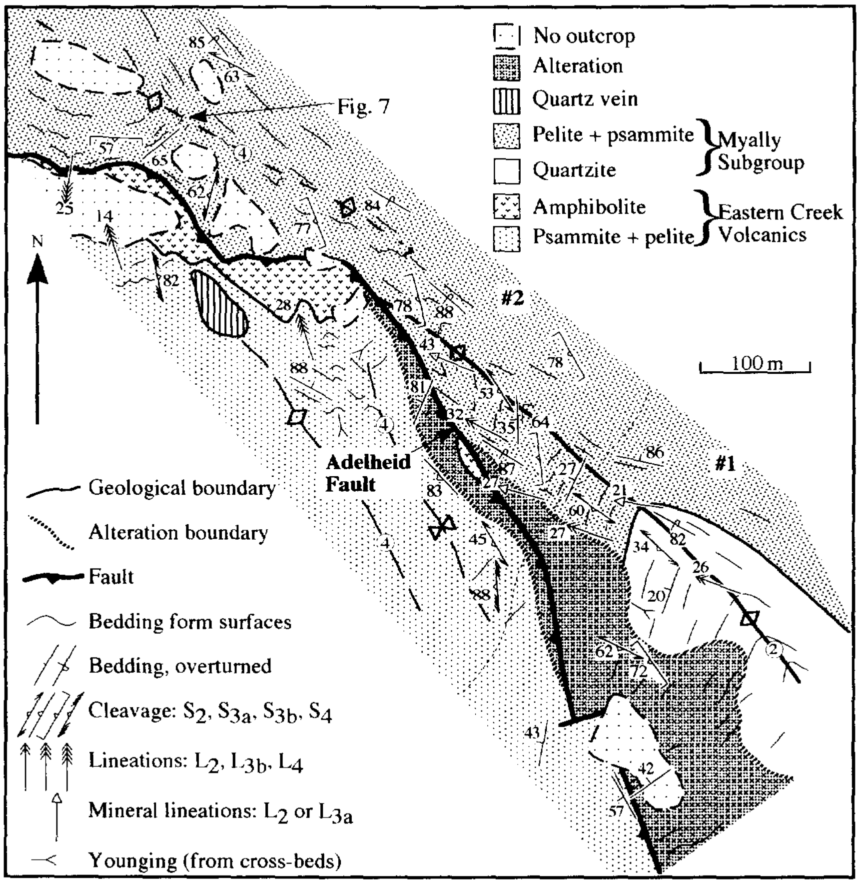

Fig. 5. Detailed map of form surfaces and overprinting relationships at key Locations 1 and 2. Note truncation of the F_2 fold by the D_{3a} Adelheid Fault. Figures 2 and 3 show that the fault is generally subparallel (or at a low angle) to bedding on the more gently W-dipping limbs of the F_2 folds, but is not repeated on the steep eastern limbs. The F_4 fold in the northwest corner of the map dies out due to interference with the older F_2 folds. See Fig. 1 for location of map.

Location 3. This area is located within the lower pelitic unit of the Myally Subgroup (Fig. 3) and is dominated by several well-developed cleavages and mesoscopic folds. In the eastern half of Location 3 (Fig. 8), S_2 is cut by a NNW- to NW-striking, weakly differentiated S_{3b} layering (Figs. 9a and 10a) which dips steeply west–southwest. In thin section, S_{3b} is defined by alternating mica rich layers (average width 3 mm) and quartz rich layers (average width 4–5 mm). Quartz grains display undulose extinction and rare subgrain development. Micas within the quartz rich domains are generally straight, and strain-free, indicating recrystallization post-S_{3b}, similar to Location 2. S_{3b} has similar orientation, style and vergence as the fabric identified as S_{3b} at Location 2.

S_{3b} is overprinted by two generations of structures (Fig. 9a). The north–south L_4 crenulations form a zonal S_4 crenulation cleavage defined by bent, deformed

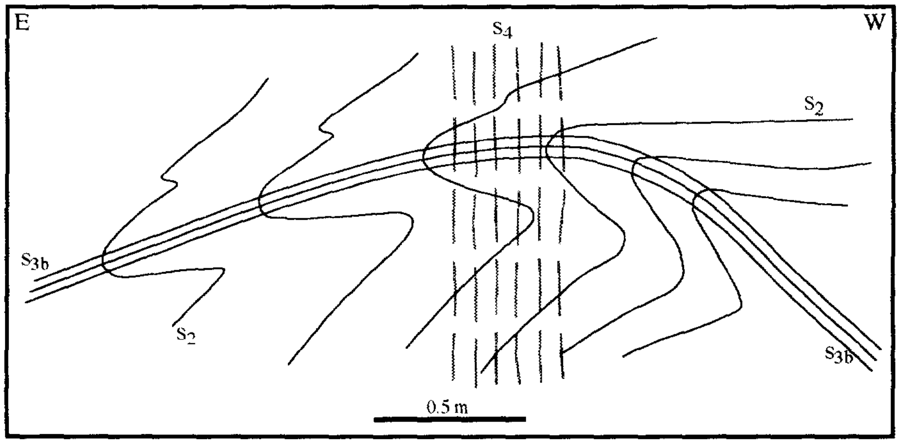

Fig. 7. Simplified outcrop sketch of overprinting relationships between S_2, S_{3b}, and S_4 from the north part of Location 2 (see Fig. 5 for outcrop location). S_2 is folded by F_{3b} and F_{3b}/S_{3b} are in turn overprinted by the upright F_4 folds and S_4 crenulation cleavage. See Figs. 6(d)–(f) for microstructures at this location.

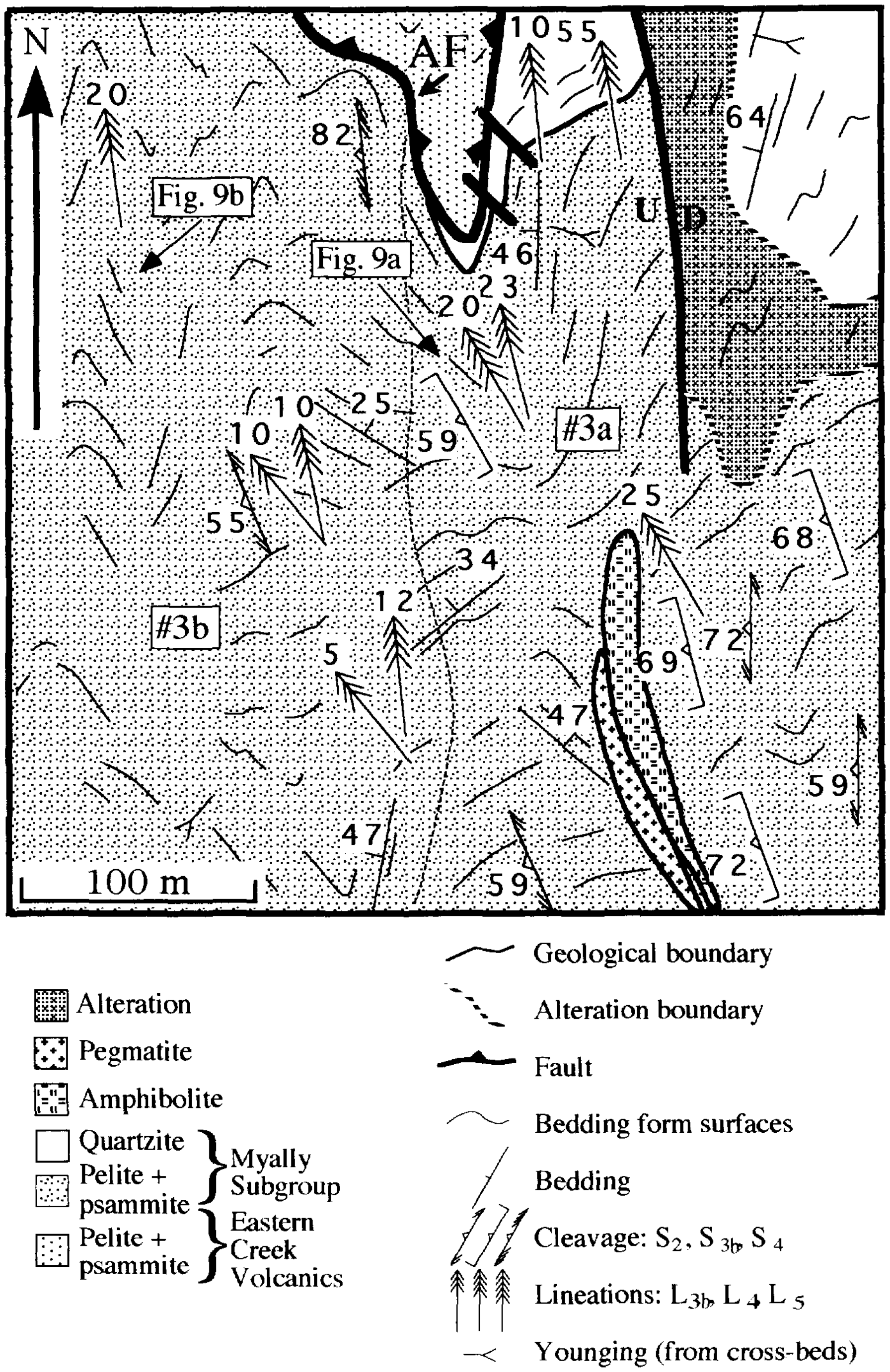

Fig. 8. Detailed map of bedding form surfaces and mesoscopic structures at Location 3. See Fig. 1 for location of map.

micas. The NW–SE-trending L_5 crenulations form a fabric only within hinge zones of F_5 folds, and they fold S_4 crenulations and cleavage (Fig. 9a). S_4 structures display a style and orientation similar to S_4 structures at Location 2.

In the western half of Location 3, the weakly differentiated S_{3b} layering is not evident. S_2 is overprinted by N-trending L_4 crenulations which form a zonal S_4 crenulation cleavage and by NW-trending folds and crenulations. In thin section, it is difficult to distinguish between the two generations of crenulations, however in rare cases one crenulation cleavage is folded by another (Fig. 10b). Clear evidence of the timing relationship comes from the preferential development of the north–south L_4 crenulations on the southwestern limbs of NW–SE-trending crenulations and folds (Fig. 9b) thereby indicating that L_4 crenulations are younger. Therefore these NW-trending structures are interpreted as F_{3b}/S_{3b}, despite the differences in style from S_{3b} in the eastern half of this location. Such variations are interpreted as reflecting temporal and/or spatial heterogeneities during deformation.

Observations from these three key locations show that although the cleavages and folds display a reasonable amount of variation in orientation and style, the sequence of structural generations can be recognized in separate parts of the study area by detailed mapping and analysis of overprinting relationships. One additional

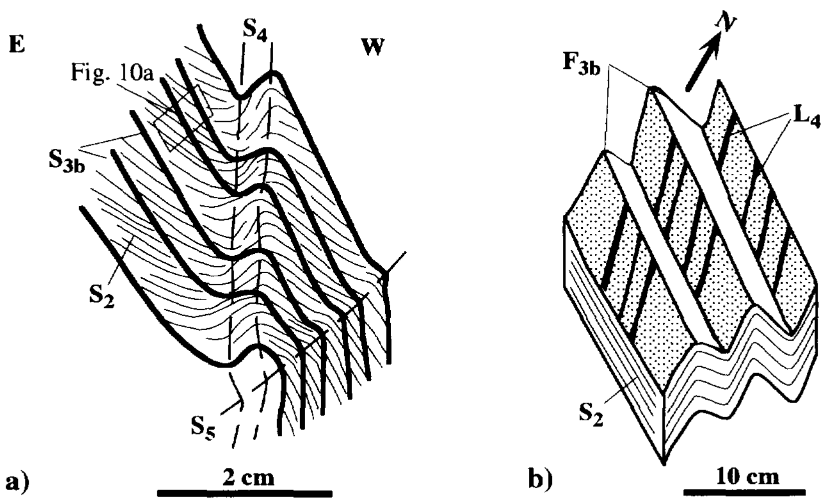

Fig. 9. (a) Outcrop sketch of overprinting relationships between S_2, differentiated S_{3b}, zonal S_4 crenulation cleavage, and L_5 crenulations. (b) Outcrop sketch depicting the preferential development of L_4 crenulations on the southwest limbs of F_{3b} folds and absence on the steeper northeast limbs. See Fig. 8 for location of outcrop sketches.

area is described in order to provide information on the Mount Isa Fault and its timing with respect to the Adelheid Fault.

Microstructure of the Mount Isa Fault mylonites

The W-dipping Mount Isa Fault separates greenschist to amphibolite facies basal Mount Isa Group equivalents from lower greenschist facies Mount Isa Group to the east (Fig. 1). In the study area, the fault occurs on the steeply overturned eastern limb of a map scale F_2 anticline (Figs. 2 and 3), but ~30 km to the north the fault cuts east into the adjacent syncline (BMR 1978).

Approaching the fault zone from the west, S_2 intensifies and parallels attenuated bedding, bedding becomes obliterated, and a strong mylonitic fabric (S_{3a}) with a steeply S- to SW-plunging mineral lineation (L_{3a}) develops. Strongly asymmetrical, highly non-cylindrical F_{3b} folds (Figs. 11a & b) with an axial planar crenulation cleavage overprint both S_2 and the S_{3a} mylonitic fabric. S_2 and the mylonites are also overprinted by a set of consistently W-dipping shear bands (Fig. 12a) which demonstrate west-over-east movement. The relative timing of shear bands and F_{3b} folds is unknown.

Microstructures and kinematic indicators of the Mount Isa Fault are similar to the Adelheid Fault. The S_{3a} mylonitic fabric of the Mount Isa Fault is defined by elongate quartz grains with slightly irregular grain boundaries and by rare micas (Figs. 12a & b). The coarser, more equant quartz grains have sutured, dentate boundaries. All grains have subgrains, deformation bands, or undulose extinction. Even the finely recrystallized, equant grains have undulose extinction and irregular boundaries, thereby indicating that recrystallization was followed by further deformation at a temperature which was insufficient for quartz recrystallization. Prismatic subgrain boundaries define '*S*' planes at an angle to the shear bands (i.e. '*C*' planes) indicating west-over-east movement. Mica fish within rare mica-rich seams also indicate E-directed displacement.

METAMORPHISM IN THE MOUNT NOVIT RANGES

Metamorphic grade in the Mount Novit Ranges varies from lower greenschist to upper amphibolite facies. Prograde metamorphic assemblages are typical of low-*P* facies metamorphism: cordierite and andalusite are common; garnet, staurolite and prograde kyanite are generally rare (cf. Yardley 1989). Geothermobarometric calculations indicate peak *P–T* conditions of approximately 600°C at 400 MPa in the western inlier (Rubenach 1992). Observation of retrograde kyanite has been interpreted to indicate isobaric cooling and an anticlockwise *P–T* path (Rubenach 1992).

Metamorphic grade increases from east to west, but the roughly north–south isograds are difficult to define due to the lack of index minerals and post-metamorphic faulting. Rocks east of the Mount Isa Fault are chlorite grade, but biotite occurs in equivalent rocks immediately west of the fault. Biotite is widely distributed in the higher grade rocks and is commonly intergrown with muscovite.

Cordierite porphyroblasts deflect S_2 and pressure shadows are developed (Fig. 13a). Internal inclusion trails (S_1?) are straight, but vary in orientation (Fig. 13a). In a sample to the northwest of this study area, S_2 cleavage traces are deflected but are continuous between the porphyroblasts and the matrix (Connors *et al.* 1992) suggesting syn-S_2 growth (cf. Vernon 1978) in agreement with Rubenach (1992). Rare andalusite porphyroblasts show similar microstructures.

Fibrolitic sillimanite forms radiating clusters, which occur in irregular patches of altered rock from centimetres to tens of metres extent, and overgrow the S_2 cleavage (Connors 1992). Near the Adelheid Fault, fibrolite clusters are stretched parallel to L_{3a} (Fig. 13b). Tensional fractures have formed perpendicular to the L_{3a} lineation (Fig. 13b) and are filled by white mica (Connors 1992). The fibrolitic sillimanite coexists with white mica in the absence of K-feldspar, but to the northwest, the peak of metamorphism is marked by late syn- to post-S_2 partial melting (Connors *et al.* 1992).

The metamorphic grade indicated by alteration assemblages associated with the Adelheid Fault helps to constrain timing of faulting with respect to metamorphism. Calc-silicate assemblages of diopside + tremolite occur in dilatant fractures that are oriented perpendicular to the L_{3a} extension lineation, and as the host to Cu mineralization (Connors 1992). In addition, veins containing assemblages of calcite + hornblende + Ca-plagioclase developed peripheral to the main diopside + tremolite core zone.

These overprinting relationships between metamorphic/metasomatic assemblages and the successive generations of cleavages help determine the timing of each cleavage generation with respect to the thermal perturbation associated with metamorphism. The implications of this are examined below.

DISCUSSION

The following discussion considers two main topics. The emphasis of the first two sections is a comparison of the structural history presented here for the Mount Novit Ranges to that of previous workers, whereas the emphasis of the subsequent sections is to consider the nature of the polyphase deformation and the factors responsible for it.

The D_1 *roof thrust hypothesis*

One of the main reasons for studying the Mount Novit Ranges was to test Bell's (1983, 1991) D_1 roof thrust hypothesis, by examining one of his key areas in more detail. The overprinting relationships of the Adelheid Fault (D_1 Meerenurker roof thrust of Bell) were carefully examined during 1:5000 scale form surface mapping and microstructural studies. In contrast, to Bell's interpretation of pre-D_2 south-directed thrusting, the evidence gathered during this study indicates that the Adelheid (Meerenurker) Fault is not folded by F_2 folds (Figs. 2 and 3) and therefore cannot be part of a pre-D_2 structure. Lineations, *S–C* fabrics, shear bands and asymmetrical folds associated with the fault all indicate west-over-east displacement, not north-over-south.

In order to account for the absence of the Adelheid (Meerenurker) Fault on the eastern limb of the F_2 fold (Figs. 2 and 3), Bell (1991) suggested that a younger fault truncated both the thrust and the F_2 anticline (see schematic map in fig. 5 of Bell 1991). This area, however, was mapped in detail during this study and no fault was found where Bell shows the 'Mount Gordon Fault' as a separate structure from the Meerenurker Thrust (compare Fig. 3 with fig. 5 of Bell). In addition, there are no obvious differences between the sections of the fault zone shown as the Meerenurker Thrust and sections interpreted as the 'Mount Gordon Fault' by Bell (1991). The entire length of the fault displays the same overprinting relationships with S_2 and F_2 structures, indicating post-F_2 movement. Although it is impossible to entirely rule out an earlier stage of movement on this fault, there is no data to support this interpretation. Similar timing relationships and sense of movement as those reported here have been documented farther north along the possible continuation of this fault zone (e.g. Huang 1990, 1991) which Bell (1991) also considers as part of his 'D_1' roof thrust.

Further evidence of post-D_2, easterly displacement on the Adelheid Fault is provided by the extension lineation in the footwall near the King prospect (see Fig. 1 for location). In proximity to the fault, radial clusters of fibrolite (Connors 1992) are stretched into elongate bundles and are pulled apart across tension fractures (Fig. 13b). Bell (1991) explained the W-plunging lineation by reorientation of his north–south D_1 lineation during reactivation of S_1 by S_2. Reorientation of a pre-S_2 lineation is precluded, however, because fibrolite grew after S_2 (see above). Mimetic growth of fibrolite over a reoriented D_1 lineation can also be ruled out by the fracturing of the fibrolite bundles which indicates that this mineral has indeed been stretched, and therefore defines a W-plunging extension lineation.

This area represented a 'keystone' to Bell's (1983, 1991) D_1 roof thrust hypothesis. The evidence presented here, however, indicates that the Adelheid (Meerenurker) Fault cannot be an early roof thrust. The validity of the entire roof thrust hypothesis and the regional significance of thrust faulting must therefore be questioned and re-evaluated. Although it is possible that local development of small scale thrust faults predated the first generation of north–south folds (i.e. F_2) in the Mount Novit Ranges, there is insufficient data to determine the nature of pre-F_2 deformation.

Timing of structural generations in the western Mount Isa Inlier

Based on supposed identification of S_1, S_2 and S_3 in separate zones of the Sybella Batholith (~1657 Ma; Connors & Page 1992, in press), Page & Bell (1986) used Rb–Sr whole rock analyses to date the three deformation events as 1610 ± 13 Ma, 1544 ± 12 Ma and 1510 ± 13 Ma, respectively. These events have, therefore, been interpreted as discrete episodes of deformation related to isolated tectonic events separated by substantial time breaks (~66 Ma and ~ 34 Ma). However, these results require re-evaluation in light of: (i) new geochronological data (Connors & Page 1992, in press); and (ii) recent geometrical and microstructural studies of cleavage development within the Sybella Batholith and country rocks (Proffett 1989, 1990, Young 1990, Davoren 1991, Connors *et al.* 1992).

New U–Pb analyses indicate that the metamorphic peak (upper amphibolite facies with local partial melting) occurred at ~1532 Ma (age of pegmatites which formed near peak metamorphism; Connors & Page, in press). Therefore, the whole-rock Rb–Sr age of 1610 ± 13 Ma obtained by Page & Bell (1986) implies that Bell's (1983) 'regional D_1' occurred ~80 Ma prior to regional metamorphism. However, it is unlikely that the Rb–Sr isotopic systems of the Sybella Batholith could be so easily reset during a D_1 event which was associated with lower greenschist facies metamorphism, and later survive upper amphibolite facies metamorphism, plastic deformation and recrystallization at ~1532 Ma, thus preserving the 1610 Ma age. Resetting of Rb–Sr isotopic systems under conditions of amphibolite facies metamorphism and plastic deformation has been documented by several studies (e.g. Georgetown Inlier, Australia, Black *et al.* 1979; Appalachians, U.S.A., Gromet 1991).

Connors & Page (in press) reassessed the 1610 Ma Rb–Sr result and suggested that several samples that may not be related to the Sybella Batholith should be excluded. The new slope indicates a Rb–Sr age of 1590 ± 55 Ma, which Connors & Page interpreted as reflecting partial resetting of Rb–Sr isotopic systems during metamorphism and plastic deformation at ~1532 Ma. They concluded (Connors & Page, in press) that this ~1590 Ma age cannot date Bell's (1983, 1991) postulated D_1 thrusting event. It is possible that all three Rb–Sr ages reflect variable resetting during deformation and metamorphism at ~1532 Ma.

The exact age of local D_1 thrust faulting is uncertain. It must have occurred between ~1626 Ma (the age of the Tommy Creek Volcanics (Hill *et al.* 1992), the youngest units affected by D_1) and ~1532 Ma (the age of peak metamorphism and F_2 folding; Connors & Page, in press). It is therefore uncertain whether early thrust faulting occurred just prior to peak metamorphism or up to ~95 Ma before.

The previous Rb–Sr age constraints that supported three distinct episodes of compressive deformation in the western Mount Isa Inlier are no longer considered valid. It is therefore interesting to consider the possibility of continuous deformation, especially given the consistent orientation and style of deformation in the Mount Novit Ranges.

Episodic vs continuous deformation

One view of structural geology is that deformation is episodic and successive generations of structural elements in polydeformed terranes formed during temporally distinct, regional deformation 'events'. The concept of overprinting structural generations, however, does not imply episodic deformation; two generations may be separated by hundreds of millions of years or may have formed during continuous deformation (e.g. Hobbs *et al.* 1976). Numerous studies in polydeformed terranes have presented evidence that deformation was continuous and that more than one generation of structures resulted during a single, progressive 'event' (e.g. Williams & Zwart 1977, Bell 1978, Quinquis *et al.* 1978, Cobbold & Quinquis 1980, Helmstaedt & Dixon 1980, Platt 1983, Ghosh & Sengupta 1984, Tobisch & Paterson 1988, Holdsworth 1990, Mawer & Williams 1991, among others).

In many examples of progressive deformation, multiple generations are largely confined to high strain zones where one or more generations of folds or cleavages are superimposed. The potentially complex overprinting relationships between these structures may give the false impression of distinct events (Tobisch & Paterson 1988, Mawer & Williams 1991). Overprinting during progressive deformation may result from changes in the orientation of the principal stress directions with respect to the early formed structures (Helmstaedt & Dixon 1980), kinematic amplification of deflections in the anisotropy (Williams & Zwart 1977, Cobbold & Quinquis 1980), or spatial variations in strain rate (Platt 1983, Holdsworth 1990).

Distinguishing between episodic and continuous deformation is not an easy task. An obvious, although typically difficult, method is to determine the absolute age of each generation. In the absence of absolute age constraints other criteria can be used. On the basis of his work in the Moine Nappe, Holdsworth (1990) outlined two main sets of criteria: (i) kinematic significance of successive structures (based on geometry, shear-sense indicators, and fold–lineation relationships); and (ii) distribution of structures in relation to variations in strain intensity (i.e. deformation partitioning). Similar criteria have been cited by other workers (e.g. Bell 1978, Quinquis *et al.* 1978, Tobisch & Paterson 1988).

In some terrains it may be possible to use the association between structural generations and metamorphic events to distinguish episodic or continuous deformation. For example, if two superimposed cleavages are defined by metamorphic minerals which are related to two distinct metamorphic events, then it is likely that the two cleavages resulted from separate tectonic episodes. The development of two or more successive generations of structures during a single metamorphic event is consistent with continuous deformation.

Although the F_2/S_2 phase of deformation and peak metamorphism in the Mount Novit Ranges is dated at ~1532 Ma (Connors 1992, Connors & Page, in press) there are no absolute age constraints on the timing of other structural generations. As a result, the evidence used in the following evaluation of episodic and continuous deformation in the Mount Novit Ranges is based in part on Holdsworth's (1990) kinematic criteria and in part on the timing relationships between polyphase deformation and regional low-P, high-T metamorphism.

Kinematics and style of deformation in the Mount Novit Ranges

The consistent asymmetry and NE- to E-vergence of F_2 folds, and attenuation of the steeply overturned east limbs, demonstrates that east–west to northeast–southwest shortening and E-directed displacement initiated during F_2. East-directed movement on post-F_2 faults and shear zones is demonstrated by the shear bands, S–C fabrics, mica fish, stratigraphic relationships and offset of metamorphic isograds. In addition, the L_{3a} mineral lineation indicates a W-plunging extension

Table 1. Summary of the geometric and kinematic characteristics of the structural generations identified in the Mount Novit Ranges

Structural generation	Fold plunge	Fold vergence	Fold style	Cleavage orientation	Stretching lineation	Faults or shear zones	Shear bands
F_2/S_2	N–WNW	NE–E	Asymmetrical	Moderate SW–W dip	Moderate to steep W–NW plunge		
Faults/shear zones	–	–		Moderate to steep ~W dip	Moderate to steep W–SW plunge	~N–S strike	west-over-east
F_{3b}-small	N–NW	NE–E	Asymmetrical	Moderate to steep W–WSW dip			
-large	~N–S	E	~Symmetrical	Steep, N–S strike			
Faulting						~N–S strike with west block up (reverse)	west-over-east
F_4/S_4	N–S	E	Symmetrical to asymmetrical	Steep, N–S strike	Very weak with steep W plunge		
Faulting						~N–S strike with west block up (reverse)	
F_5/S_5	NW	?	~Symmetrical	Weak, NW strike			

direction (see Table 1 for a summary of the kinematic indicators and the orientation of structures).

The preferential development of some faults/shear zones on the overturned, attenuated limbs of F_2 folds (Fig. 2) suggests that west-over-east displacement during faulting was localized, in part, in S_2 high strain zones. This localization of deformation and the similar kinematics are consistent with continuous deformation, and suggest large scale partitioning of deformation with time. In addition, the local difficulties in distinguishing S_2 from S_{3a} or S_{3b}, are consistent with contemporaneous development and therefore favor progressive deformation (cf. Tobisch & Paterson 1988).

The localization of non-cylindrical F_{3b} folds, along with their geometry and orientation, suggests that they formed as a result of continued E-directed movement along the faults and shear zones (cf. Bell 1978, Quinquis *et al.* 1978; Cobbold & Quinquis 1980, Ghosh & Sengupta 1984, Holdsworth 1990, Mawer & Williams 1991). The progression from strongly asymmetrical folds with inclined axial planes to more upright symmetrical F_{3b} folds, and decreasing intensity of S_{3b}, with increasing distance from the faults, further supports a genetic relationship.

Continued west-over-east faulting is demonstrated by truncation of F_{3b} folds by both the Mica Creek Shear Zone and Big Beryl Fault which are exposed ~15 km to the north of this study area (Proffett 1989, 1990, Connors *et al.* 1991, 1992), and by microstructural evidence (i.e. preservation of *S–C* fabrics and shear bands, and lack of annealing and grain growth in quartz; Figs. 6c, 12a & b) which indicates continued displacement on the faults during and after F_{3b}/S_{3b}. Persistence of this same kinematic framework is further supported by the orientation and large scale asymmetry of F_4 folds (Figs. 2 and 4), and west-over-east movement on steep, post-F_4 faults (e.g. Snowy Fault; Fig. 2).

The consistent kinematic framework during F_2 folding, ductile faulting, F_{3b} folding, further movement on faults and shear zones, F_4 folding, and further faulting (Table 1) suggests that this succession of structures formed during a single, continuous tectonic event. Although each generation of structures may represent a 'pulse' of deformation, the similar kinematic framework is more consistent with nearly continuous deformation than with discrete, unrelated episodes of deformation.

Metamorphic conditions during polyphase deformation

The progressive variation in metamorphic conditions during polyphase deformation produced distinct textural variations between the successive cleavage generations as the thermal conditions peaked and subsided (Fig. 14). The porphyroblast–matrix relationships (Fig. 13a) indicate that the temperature was sufficient for pre- to syn-S_2 growth of andalusite and syn-S_2 growth of cordierite (cf. Vernon 1978). Formation of cordierite indicates that the temperature reached approximately 500°C during S_2, assuming a pressure of 300–400 MPa (Brown *et al.* 1988).

Microstructures dominated by minimum surface energy textures (Vernon 1976) in quartz and mica grains defining S_2 (e.g. granoblastic and decussate, respectively; Fig. 6a) indicate that temperature was sufficient to allow recrystallization (surface energy dominated grain boundary migration) and that the thermal event outlasted the deformation phase that produced the S_2 cleavage (e.g. Williams *et al.* 1977). Decussate mica textures such as those defining S_2 are interpreted to develop by kinking plus kind-boundary migration and recrystallization (Williams *et al.* 1977) and provide evidence of a pre-S_2 fabric.

Peak metamorphism is defined by radial fibrolite clusters which grew late syn- to post-S_2, but predated

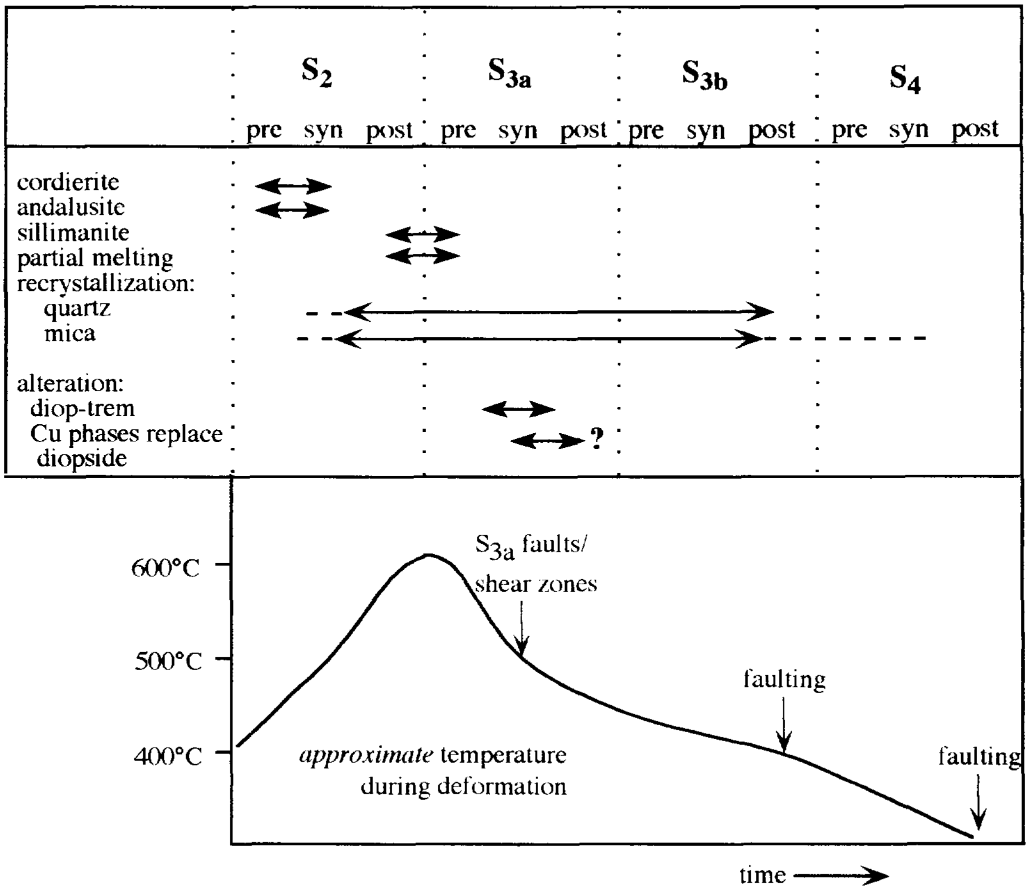

Fig. 14. Diagram summarizing the relative timing of deformation phases and low-P, high-T metamorphism. Estimated temperatures are based on metamorphic and metasomatic assemblages associated with each deformation phase and are *not* well constrained.

ductile faulting. The stability of sillimanite + muscovite in the absence of K-feldspar suggests a peak temperature of approximately 600°C at a pressure of 300–400 MPa (Brown *et al.* 1988). Near the Adelheid Fault, fibrolite clusters are stretched parallel to L_{3a} without significant retrogression, therefore indicating that faulting/shearing post dates the metamorphic peak, but that metamorphic conditions remained within the sillimanite stability field. In addition, formation of diopside and diopside + tremolite assemblages in extensional fractures associated with the Adelheid Fault (Connors 1992) suggests temperature was in the range of 450–550°C based on the P–T–X data of Slaughter *et al.* (1975). Associated calc-silicate veins containing calcite + hornblende + Ca-plagioclase also indicate amphibolite facies conditions (e.g. Yardley 1989) during faulting.

Despite these elevated temperatures, quartz microstructures associated with S_{3a} in the Adelheid and Mount Isa Faults show no evidence of post-tectonic annealing (Figs. 6c, 12a & b). Thus strain persisted in these fault zones until temperature was insufficient for annealing and grain growth (i.e. S_4 time). Mylonites of the Mount Isa Fault preserve evidence of rotation recrystallization (i.e. fine, prismatic grains and subgrains) which produced new grains that in turn accumulated further strain and recrystallized by grain boundary migration during continued deformation and dynamic recrystallization (e.g. Urai *et al.* 1986).

The temperature declined progressively from S_{3a} to S_{3b} to S_4 (Fig. 14) until conditions were insufficient for recrystallization and annealing of quartz. Micas defining S_{3b} are largely recrystallized (Figs. 6d & e and 10a), but the laths are thin and elongate in comparison to the broad laths that define S_2 (Figs. 6a & b), and the quartz grains defining S_{3b} are strained. Pseudomorphs of white mica after fibrolite are overprinted by S_4 (or S_{3b}?), thus retrogression probably began before S_4 time. In rocks where S_4 is well developed, quartz grains are strained and show no evidence of annealing, and micas are generally bent and strained (Fig. 6f). S_5 fabrics show no evidence of recrystallization of either quartz or mica.

The progressive variation in mineral assemblages and microstructures associated with the succession of deformation phases, documents development of these structures during the thermal rise and decline associated with regional low-pressure metamorphism (Fig. 14). This implies that: (i) F_2/S_2, S_{3a}/L_{3a}, F_{3b}/S_{3b}, and F_4/S_4 ($+F_5/S_5$) all developed during a single thermal pulse (Fig. 14); and (ii) that these deformation phases formed within the period of time required for the regional low-P, high-T metamorphic event.

Although the duration of this metamorphic event is not known, the development of low-P facies assemblages rather than medium-P facies has implications for the duration of the event. Modelling of thermal reequilibration after crustal thickening (England & Thompson 1984) shows that rocks spend 30–50% of their time (~20–40 Ma) near their peak T conditions, however, this applies only to medium-P facies metamorphism. In contrast, numerous recent studies of low-P metamorphism have shown that crustal thickening cannot account for high-T at shallow crustal levels and that an additional heat source is required. Heat advection due to migration of melts to mid-crustal levels has been proposed to explain low-P metamorphism during crustal thickening in the Mount Isa Inlier (Connors 1992, Rubenach 1992). Modelling of a thermal perturbation such as this suggests that the resulting metamorphic event will be short-lived ($\ll$1 Ma; e.g. Jaeger 1964, Lux *et al.* 1986, Wickham & Oxburgh 1987, Barton & Hanson 1989, De Yoreo *et al.* 1989, Buntebarth 1991, Furlong *et al.* 1991, among others) in distinct contrast to medium-P rocks (~20–40 Ma). Periodic emplacement of additional magma may, however, prolong the thermal perturbation.

Regardless of the duration, it can generally be assumed that a consistent tectonic regime prevailed throughout the thermal event. It is unlikely that low-P, high-T metamorphism, related to emplacement of magmas in the mid-crust, would persist through two separate tectonic events such as the 'regional' D_2 and D_3 of Bell (1983, 1991) that are interpreted to occur 34 Ma apart. Thus the temporal association between the successive structural generations and low-P, high-T metamorphism, provides further evidence that the deformation phases occurred during a single tectonic event, not as a series of discrete events separated by significant time breaks.

Episodic or continuous deformation?

The kinematic and metamorphic relationships described in the previous two sections indicate that polyphase deformation in the Mount Novit Ranges occurred within a consistent tectonic regime and within the time required for decay of the thermal perturbation associated with low-P metamorphism. This indicates that episodic deformation related to distinct tectonic events could not have been responsible for the polyphase deformation in the Mount Novit Ranges. It is possible, however, that the polyphase deformation resulted from distinct pulses of deformation during the single tectonic event. Therefore, based on the definition of continuous deformation provided by other workers (see above), polyphase deformation in the Mount Novit Ranges may not have been *truly* continuous, although it probably was nearly continuous. Regardless, the temporal constraints provided by the relationships between deformation and low-P metamorphism, imply that polyphase deformation occurred within a time period substantially shorter than that generally attributed to regional deformation and metamorphism associated with crustal thickening and thermal reequilibration of an overthickened crust.

Factors responsible for polyphase deformation

The Mount Novit Ranges are bounded to the west by the relatively competent Sybella buttress and to the east by the Mount Isa Fault (Figs. 1 and 15). The Sybella buttress is interpreted to represent a significant structure in the western Mount Isa Inlier which has strongly influenced strain distribution and orientation of structures during ~east–west shortening (Connors 1992). Several major faults or fault systems die out or change orientation approaching the buttress (Connors 1992). For example, dip-slip movement on the Mount Isa Fault may be partly translated into strike-slip motion north of the buttress and the May Downs fault system appears to die out to the south and/or merge with the Mount Isa Fault (Fig. 1 inset). The Sybella buttress consists of thick, competent quartzite of the Mount Guide Quartzite, amphibolite of the Eastern Creek Volcanics, and the sheet-like metagranite of the ~1657 Ma Sybella Batholith (Connors & Page 1992, in press) which intrudes these units (Figs. 15a & b) and predates compressional deformation. The zone of more intense deformation in the Mount Novit Ranges dies out to the north where outcrop of the granite body plunges beneath the present erosion surface.

During polyphase deformation the interbedded metasediments and metavolcanics accommodated more strain than the thick layers of granite, quartzite, and amphibolite. The most obvious factor involved is the greater competency of the granite + quartzite + amphibolite block in comparison to the thinly interlayered metasediments and amphibolites of the Mount Novit Ranges. Initial strain localization may have induced further weakening and continued strain concentration.

Although the buttress acted as a more competent block during much of the shortening history, the effects of some deformation phases are well developed. S_2 occurs throughout the metagranite, especially in finer grained zones, and it is overprinted by large scale F_{3b} (or F_4) folds (Figs. 15a & b) which generally lack an axial plane cleavage (Connors *et al.* 1992). The faults and shear zones which are widespread in the Mount Novit Ranges, are not evident within the buttress. Thus the buttress has accommodated part of the strain during some stages of polyphase deformation; however the effects of other deformation phases, especially faulting, are concentrated in the Mount Novit Ranges.

As polyphase deformation continued in the Mount Novit Ranges, the influx of fluids during faulting is likely to have further weakened this zone, promoting continued localization of strain. In addition, retrograde alteration produced phyllosilicate-rich assemblages in originally more competent units further weakening these zones.

Thus this succession of structures in the Mount Novit Ranges resulted from a combination of local effects, and therefore does not necessarily reflect the regional

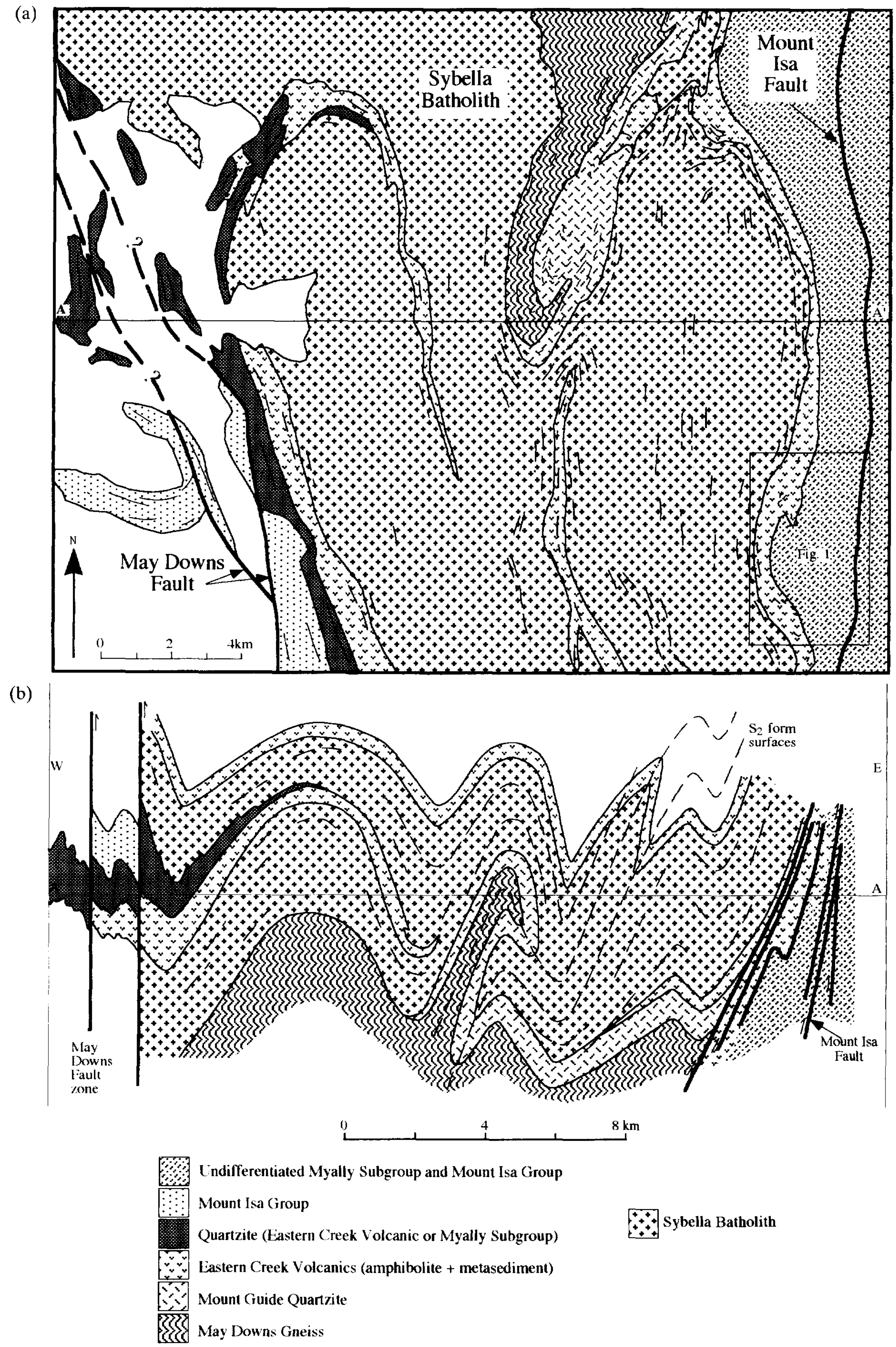

Fig. 15. (a) Simplified map of part of the Sybella buttress depicting distribution of thick competent units of metagranite, quartzite, and amphibolite between the Mount Isa and May Downs faults (modified from BMR 1978). The location of Fig. 1 is indicated. (b) Simplified cross-section across the Sybella buttress showing interpreted structure of the thick, competent sheet of metagranite and its relationship to the intensely deformed Mount Novit Ranges. The overall degree of deformation is much higher in the less competent zone of the Mount Novit Ranges. See Figs. 2 and 3 for detailed structure of the Mount Novit Ranges.

structures. Although the effects of this east–west to northeast–southwest period of shortening are evident across the inlier, the resulting assemblage of structures varies. For example, the same sequence of structures could not be identified in the lower grade rocks east of the Mount Isa Fault (Connors *et al.* 1991, 1992). Heterogeneous deformation may have resulted from various effects such as pre-existing structures, variations in rock types and their distribution, syn-deformational temperature gradients, fluid activity and/or alteration. This period of east–west to northeast–southwest shortening in the Mount Novit Ranges appears to correlate with Bell's (1983, 1991) D_2 and D_3.

CONCLUSIONS

(1) There is little evidence for D_1 deformation in the Mount Novit Ranges. Evidence of a pre-S_2 fabric is found only in thin section as relict crenulations within S_2 microlithons and as inclusion trails within porphyroblasts. No F_1 folds were identified. Bell's (1991) postulated south-directed D_1 Meerenurker roof thrust with >250 km, is a post-F_2 fault with easterly displacement. General applicability of Bell's (1991) model must therefore be reassessed.

(2) The Mount Novit Ranges have experienced polyphase deformation resulting in four fold/cleavage generations and several stages of intermittent faulting and shearing which reflect ~east–west to northeast–southwest shortening and E-directed displacement. Asymmetrical F_2 folds were followed by ductile faults/shear zones with easterly displacement. Strongly asymmetrical, non-cylindrical F_{3b} folds developed adjacent to the faults/shear zones, while more symmetrical, upright F_{3b} folds formed elsewhere. Further shortening resulted in intermittent fault activity and F_4 ($\pm F_5$) folds.

(3) This succession of structural generations formed during regional low-P, high-T metamorphism. Prograde metamorphism occurred syn-S_2, and elevated temperatures sufficient for recrystallization of micas and quartz outlasted S_2 formation and continued through to S_{3a} and S_{3b} time. Metamorphic conditions waned and by S_4 time, recrystallization and grain growth no longer took place during deformation.

(4) The kinematic, geometric and spatial relationships between all of the structural generations support development of the entire succession within a consistent tectonic regime. Further support is demonstrated by development of these structural generations during the thermal rise and decline associated with low-P, high-T metamorphism. These observations are more consistent with continuous, progressive deformation than with isolated tectonic episodes.

(5) The dominant factor responsible for the intensity of polyphase deformation in the Mount Novit Ranges, at least initially, was the thick block of competent metagranite, quartzite, and amphibolite to the west which accommodated less strain during much of the deformation history. Once strain was localized in the Mount Novit Ranges, the development of faults/shear zones and the associated alteration may have further weakened this zone, enhancing the likelihood of continued strain localization.

(6) The D_1–D_2–D_3 scheme of the Mount Isa Inlier is insufficient and may lead to inaccurate correlations. Deformation has been heterogeneous on all scales and multiple generations of structures have developed in high strain zones such as the Mount Novit Ranges. The variations in style and orientation within a single generation of structures, and the similarity in style and orientation in successive structural generations demonstrates the inherent problems in relying on these characteristics to correlate structural generations in the absence of detailed geometrical analyses and form surface mapping.

Acknowledgments—We would like to thank June Hill, Rob Scott and Nick Oliver for valuable input during the 1988 and 1989 Monash Earth Science undergraduates field camps; John Proffett, Bill Perkins and Mike Rickard for stimulating discussions in the field; Paul Williams, Simon Hanmer, Tim Bell, Colin Winsor, John Platt and Colleen Elliott for reviewing various drafts of the manuscript; and Draga Gelt for drafting Fig. 3. We gratefully acknowledge the Australian Geological Survey Organization for logistical support, air photos, and air photo enlargements provided during the 1988 and 1989 field seasons and Mount Isa Mines for air photo enlargements, orthophotos and accommodation during the 1990 field season. KAC was funded by a 1967 Natural Sciences and Engineering Research Council of Canada Postgraduate Scholarship and in part by Mount Isa Mines. Some support for this project was also provided by an Australian Research Council grant 'Continental Extension Tectonics' to GSL.

REFERENCES

Bain, J. H. C., Heinrich, C. A. & Henderson, G. A. M. 1992. Stratigraphy, structure and metasomatism of the Haslingden Group, east Moondarra area, Mount Isa: a deformed and mineralized Proterozoic multistage rift-sag sequence. In: *Detailed Studies in the Mount Isa Inlier* (edited by Stewart, A. J. & Blake, D. H.). *Bull. Aust. Geol. Survey Organisation* **243**, 125–136.

Barton, M. D. & Hanson, P. B. 1989. Magmatism and the development of low-pressure metamorphic belts: implications from the western United States and thermal modeling. *Bull. geol. Soc. Am.* **101**, 1051–1065.

Bell, T. H. 1978. Progressive deformation and reorientation of fold axes in a ductile mylonite zone: the Woodroffe thrust. *Tectonophysics* **44**, 285–321.

Bell, T. H. 1983. Thrusting and duplex formation at Mount Isa, Queensland, Australia. *Nature* **304**, 493–497.

Bell, T. H. 1991. The role of thrusting in the structural development of the Mount Isa Mine and its relevance to exploration in the surrounding region. *Econ. Geol.* **86**, 1602–1625.

Bell, T. H., Reinhardt, J. & Hammond, R. J. 1992. Multiple foliation development during thrusting and synchronous vertical shear zone development. *J. Struct. Geol.* **14**, 791–805.

Black, L. P., Bell, T. H., Rubenach, M. J. & Withnall, L. W. 1979. Geochronology of discrete structural–metamorphic events in a multiply deformed Precambrian terrane. *Tectonophysics* **54**, 103–137.

Blake, D. H. 1987. Geology of the Mount Isa Inlier and environs, Queensland and Northern Territory. *Bull. Bur. Miner. Resources, Aust.* **225**.

Blake, D. H. 1992. Stratigraphy, folding and faulting within the Quilalar Fault System, Mount Isa Inlier. In: *Detailed Studies in the Mount Isa Inlier* (edited by Stewart, A. J. & Blake, D. H.). *Bull. Aust. Geol. Survey Organisation* **243**, 161–179.

BMR, 1978. Mount Isa 1:100 000 Geological Series, Sheet 6756.

Brown, T. H., Berman, R. G. & Perkins, E. H. 1988. Ge0-Calc: Software package for calculation and display of pressure–

temperature–composition phase diagrams using an IBM or compatible personal computer. *Comput. Geosci.* **14**, 279–289.

Buntebarth, G. 1991. Thermal models of cooling. In: *Equilibrium and Kinetics in Contact Metamorphism: The Ballachulish Igneous Complex* (edited by Voll, G., Topel, J., Pattison, D. R. M. & Siefert, F.). Heidelberg, Springer-Verlag, 379–402.

Carter, E. K., Brooks, J. M. & Walker, K. R. 1961. The Precambrian mineral belt of northwestern Queenland. *Bull. Bur. Miner. Resources, Aust.* **51**, 344.

Cobbold, P. R. & Quinquis, H. 1980. Development of sheath folds in shear regimes. *J. Struct. Geol.* **2**, 119–126.

Connors, K. A. 1989. Implications of an early fold/thrust event in the western Mount Isa Inlier. Australasian Tectonics, Kangaroo Island Conference. *Abs. Geol. Soc. Aust.* **24**, 25–26.

Connors, K. A. 1992. Tectonothermal evolution of the Mount Novit Ranges, Mount Isa Inlier, Australia. Unpublished Ph.D. thesis, Monash University, Melbourne, Australia.

Connors, K. A. & Page, R. W. 1992. Age relationships between granite intrusion, metamorphism, and deformation in the Mount Isa Inlier. *Abs. Geol. Soc. Aust.* **32**, 229–230.

Connors, K. A. & Page, R. W. In Press. Geochronology of magmatism, metamorphism, and deformation in the western Mount Isa Inlier. *Precambrian Res.* **71**.

Connors, K. A., Proffett, J. M. Lister, G. S., Scott, R. J., Oliver, N. H. S. & Young, D. J. 1991. Geology of the Mount Novit Ranges 1:25 000 map sheet. *Bull. Aust. Geol. Survey Organisation.*

Connors, K. A., Proffett, J. M., Lister, G. S., Scott, R. J., Oliver, N. H. S. & Young, D. J. 1992. Geology of the Mount Novit Ranges, southwest of Mount Isa Mine. In: *Detailed Studies in The Mount Isa Inlier* (edited by Stewart, A. J. & Blake, D. H.). *Bull. Aust. Geol. Survey Organisation* **243**, 137–160.

Davoren, P. J. 1991. A structural, metamorphic and metasomatic study of an area west of the Mount Isa Fault, Mount Isa, Northwest Queensland. Unpublished Honours thesis, Monash University, Melbourne, Australia.

Derrick, G. M. 1982. A Proterozoic rift zone at Mount Isa, Queensland, and implications for mineralization. *BMR J. Aust. Geol. Geophys.* **7**, 81–92.

De Yoreo, J. J., Lux, D. R. & Guidotti, C. V. 1989. The role of crustal anatexis and magma migration in the thermal evolution of regions of thickened continental crust. In: *Evolution of Metamorphic Belts* (edited by Daly, J. S., Cliff, R. A. & Yardley, B. W. D.) *Spec. Publ. geol. Soc.* **43**, 187–202.

Downing, J. G. 1986. Structural and metamorphic geology of the Mica Creek area, Mount Isa, northwest Queensland. Unpublished Honours thesis, James Cook University, Townsville, Australia.

Dunnet, D. 1976. Mount Isa—reconstruction of a faulted ore-body. *Phil. Trans. R. Soc. Lond., Series A* **283**, 333–344.

England, P. C. & Thompson, A. B. 1984. Pressure–temperature–time paths of regional metamorphism I. Heat transfer during the evolution of regions of thickened continental crust. *J. Petrol.* **25**, 894–928.

Furlong, K. P., Hanson, R. B. & Bowers, J. R. 1991. Modeling thermal regimes. In: *Contact Metamorphism* (edited by Kerrick, D. M.). *Miner. Soc. Am.* **26**, 437–506.

Ghosh, S. K. & Sengupta, S. 1984. Successive development of plane noncylindrical folds in progressive deformation. *J. Struct. Geol.* **6**, 703–709.

Gray, D. R. 1977. Morphological classification of crenulation cleavages. *J. Geol.* **85**, 229–235.

Gromet, L. P. 1991. Direct dating of deformational fabrics. In: *Applications of Radiogenic Isotope Systems to Problems in Geology, Short Course Handbook* (edited by Heaman, L. & Ludden, J. N.). *Miner. Assoc. Can.* **19**, 167–189.

Helmstaedt, H. & Dixon, J. M. 1980. Superposed crenulation cleavages resulting from progressive deformation. *Tectonophysics* **66**, 115–126.

Hill, E. J., Loosveld, R. J. H. & Page, R. W. 1992. Structure and geochronology of the Tommy Creek Block, Mount Isa Inlier. In: *Detailed Studies in the Mount Isa Inlier* (edited by Stewart, A. J. & Blake, D. H.). *Bull. Aust. Geol. Survey Organisation* **243**, 329–348.

Hill, R. M., Wilson, I. H., Derrick, G. M. & Mitchell, J. E. 1975. Geology of the Mount Isa 1:100 000 Sheet area, northwest Queensland. Bureau Miner. Resources, Aust., Record 1975/175.

Hobbs, B. E., Means, W. D. & Williams, P. F. 1976. *An Outline of Structural Geology*. John Wiley & Sons, New York.

Holcombe, R. J., Pearson, P. J. & Oliver, N. H. S. 1991. Geometry of a middle Proterozoic extensional décollement in northeastern Australia. *Tectonophysics* **191**, 255–274.

Holcombe, R. J. & Stewart, A. J. 1992. Note on deformation terminology. In: *Detailed Studies in the Mount Isa Inlier* (edited by Stewart, A. J. & Blake, D. H.). *Bull. Aust. Geol. Survey Organisation* **243**, 13–14.

Holdsworth, R. E. 1990. Progressive deformation structures associated with ductile–thrusts in the Moine Nappe, Sutherland, N. Scotland. *J. Struct. Geol.* **12**, 443–452.

Huang, W. 1990. Geology west of Mount Isa Mines. Mount Isa Mines, unpublished report.

Huang, W. 1991. A note on the microstructures within and along the western section of the 'Growth Fault'. Mount Isa Mines, unpublished report.

Jaeger, J. C. 1964. Thermal effects of intrusions. *Rev. Geophys. & Space Phys.* **2**, 443–466.

Lister, G. S. 1969. Aspects of metamorphism and structure across the Mount Isa Fault in the Mount Novit area. Unpublished Honours thesis, University College of Townsville, Townsville, Australia.

Loosveld, R. J. H. 1992. Structural geology of the central Soldiers Cap Belt, Mount Isa Inlier, Australia. In: *Detailed Studies in the Mount Isa Inlier* (edited by Stewart, A. J. & Blake, D. H.). *Bull. Aust. Geol. Survey Organisation* **243**, 349–360.

Loosveld, R. & Schreurs, G. 1987. Discovery of thrust klippen, northwest of Mary Kathleen, Mt Isa Inlier, Australia. *Aust. J. Earth Sci.* **34**, 387–402.

Lux, D. R., De Yoreo, J. J., Guidotti, C. V. & Decker, E. R. 1986. Role of plutonism in low-pressure metamorphic belt formation. *Nature* **323**, 794–797.

Mawer, C. K. & Williams, P. F. 1991. Progressive folding and foliation development in a sheared, coticule-bearing phyllite. *J. Struct. Geol.* **13**, 539–555.

Nijman, W., Mijnlieff, H. F. & Schalkwijk, G. S. 1992. The Hero fan delta (lower Mount Isa Group) and its structural control: deformation in the Hero/Western Fault zones and Paroo Range compared, Mount Isa Inlier, Queensland, Australia. In: *Detailed Studies in the Mount Isa Inlier* (edited by Stewart, A. J. & Blake, D. H.). *Bull. Aust. Geol. Survey Organisation* **243**, 75–110.

Oliver, N. H. S., Holcombe, R. J., Hill, E. J. & Pearson, P. J. 1991. Tectono-metamorphic evolution of the Mary Kathleen Fold Belt, northwest Queensland: A reflection of mantle plume processes? *Aust. J. Earth Sci.* **38**, 425–455.

Page, R. W. & Bell, T. H. 1986. Isotopic and structural responses of granite to successive deformation and metamorphism. *J. Geol.* **94**, 365–379.

Passchier, C. W. 1986. Evidence for early extensional tectonics in the Proterozoic Mount Isa Inlier, Australia. *Geology* **14**, 1008–1011.

Passchier, C. W. & Williams, P. F. 1989. Proterozoic extensional deformation in the Mount Isa Inlier, Queensland, Australia. *Geol. Mag.* **126**, 43–53.

Pearson, P. J., Holcombe, R. J. & Oliver, N. H. S. 1987. The Mary Kathleen Fold Belt, northwest Queensland: D_1—a product of crustal extension. International Conference on the Deformation of Crustal Rocks, Mt Buffalo, Australia. *Abs. Geol. Soc. Aust.* **19**, 37–38.

Pearson, P. J., Holcombe, R. J. & Page, R. W. 1992. Synkinematic emplacement of the Middle Proterozoic Wonga Batholith into a mid-crustal extensional shear zone, Mount Isa Inlier, Queenland, Australia. In: *Detailed Studies in the Mount Isa Inlier* (edited by Stewart, A. J. & Blake, D. H.). *Bull. Geol. Survey Organisation* **243**, 289–328.

Platt, J. P. 1983. Progressive refolding in ductile shear zones. *J. Struct. Geol.* **5**, 619–622.

Proffett, J. M. 1989. Progress report, geological mapping in the Mount Isa district, Queensland. Mount Isa Mines Ltd., unpublished report.

Proffett, J. M. 1990. Some new observations on the geologic structure southwest of Mount Isa. *Mt Isa Inlier Geol. Conf. Abs.*, Monash University, Melbourne, 29–31.

Quinquis, H., Audren, C., Brun, J. P. & Cobbold, P. R. 1978. Intense progressive shear in Ile de Groix Blueschists and compatibility with subduction or obduction. *Nature* **273**, 43–45.

Rubenach, M. J. 1992. Proterozoic low-pressure/high-temperature metamorphism and anti-clockwise *P-T-t* path for the Hazeldene area, Mount Isa Inlier, Queensland, Australia. *J. Metamorph. Geol.* **10**, 333–346.

Slaughter, J., Kerrick, D. M. & Wall, V. J. 1975. Experimental and thermodynamic study of equilibria in the system $CaO–MgO–SiO_2–H_2O–CO_2$. *Am. J. Sci.* **275**, 143–162.

Smith, W. D. 1969. Penecontemporaneous faulting and its likely significance in relation to Mount Isa ore deposition. *Spec. Publ. geol. Soc. Aust.* **2**, 225–235.

Stewart, A. J. 1989. Extensional faulting as the explanation for the Deighton 'Klippe' and other Mount Albert Group outliers, Mount

Isa Inlier, northwestern Queensland. *Aust. J. Earth Sci.* **36**, 405–421.

Stewart, A. J. 1992a. Stratigraphy, extension, and contraction in the Ballara-Mount Frosty area, Mount Isa Inlier, Queensland. In: *Detailed Studies in the Mount Isa Inlier* (edited by Stewart, A. J. & Blake, D. H.). *Bull. Aust. Geol. Survey Organisation* **243**, 209–228.

Stewart, A. J. 1992b. Geology of the Horse's head structure, north of Mount Isa, and its bearing on the 'roof thrust + imbricate stack' hypothesis. Mount Isa Inlier, Queensland. In: *Detailed Studies in the Mount Isa Inlier* (edited by Stewart, A. J. & Blake, D. H.). *Bull. Aust. Geol. Survey Organisation* **243**, 111–124.

Tobisch, O. T. & Paterson, S. R. 1988. Analysis and interpretation of composite foliations in areas of progressive deformation. *J. Struct. Geol.* **10**, 745–754.

Urai, J. L., Means, W. D. & Lister, G. S. 1986. Dynamic recrystallization of minerals. In: *Mineral and Rock Deformation: Laboratory Studies. Geophys. Monograph* **36**, Am. Geophys. Union, 161–199.

Vernon, R. H. 1976. *Metamorphic Processes*. George Allen & Unwin Ltd., London.

Vernon, R. H. 1978. Porphyroblast-matrix relationships in deformed metamorphic rocks. *Geol. Rdsch.* **67**, 288–305.

Wickham, S. M. & Oxburgh, E. R. 1987. Low pressure regional metamorphism in the Pyrenees and its implications for the thermal evolution of rifted continental crust. *Phil. Trans. R. Soc. Lond.* **A 321**, 219–242.

Williams, P. F. 1970. Structure of the Mount Isa District. Mount Isa Mines Limited, unpublished report.

Williams, P. F. & Zwart, H. J. 1977. A model for the development of the Seve-Köli Caledonian nappe complex. In: *Energetics of Geological Processes* (edited by Saxena, S. K. & Bhattacharji, S.). Springer, New York, 169–187.

Williams, P. F., Means, W. D. & Hobbs, B. E. 1977. Development of axial-planar slaty cleavage and schistosity in experimental and natural materials. *Tectonophysics* **42**, 139–158.

Williams, P. R. 1989. Nature and timing of early extensional structures in the Mitakoodi Quartzite, Mount Isa Inlier, northwest Queensland. *Aust. J. Earth Sci.* **36**, 283–296.

Wilson, C. J. L. 1972. The stratigraphic and metamorphic sequence west of Mount Isa, and associated igneous intrusions. *Proc. Australas. Inst. Min. and Metall.* **243**, 27–42.

Wilson, C. J. L. 1973. Faulting west of Mount Isa mine. *Proc. Australas. Inst. Min. and Metall.* **245**, 3–15.

Wilson, C. J. L. 1975. Structural features west of Mount Isa. *J. Geol. Soc. Aust.* **22**, 457–476.

Winsor, C. N. 1986. Intermittent folding and faulting in the Lake Moondarra area, Mount Isa, Queensland. *Aust. J. Earth Sci.* **33**, 27–42.

Yardley, B. W. D. 1989. *An Introduction to Metamorphic Petrology*. Longman Scientific & Technical, Essex.

Young, D. J. 1990. Aspects of structure and metamorphism of the vortex, Mount Isa. Unpublished M.Sc. preliminary thesis, Monash University, Melbourne, Australia.